# Fusion probability in heavy nuclei

Tathagata Banerjee,[1] S. Nath,[1,*] and Santanu Pal[2,†]

[1]*Nuclear Physics Group, Inter University Accelerator Centre, Aruna Asaf Ali Marg, Post Box 10502, New Delhi 110067, India*
[2]*CS-6/1, Golf Green, Kolkata 700095, India*

**Background:** Fusion between two massive nuclei is a very complex process and is characterized by three stages: (a) capture inside the potential barrier, (b) formation of an equilibrated compound nucleus (CN), and (c) statistical decay of the CN leading to a cold evaporation residue (ER) or fission. The second stage is the least understood of the three and is the most crucial in predicting yield of superheavy elements (SHE) formed in complete fusion reactions.

**Purpose:** A systematic study of average fusion probability, $\langle P_{CN} \rangle$, is undertaken to obtain a better understanding of its dependence on various reaction parameters. The study may also help to clearly demarcate onset of non-CN fission (NCNF), which causes fusion probability, $P_{CN}$, to deviate from unity.

**Method:** ER excitation functions for 52 reactions leading to CN in the mass region 170–220, which are available in the literature, have been compared with statistical model (SM) calculations. Capture cross sections have been obtained from a coupled-channels code. In the SM, shell corrections in both the level density and the fission barrier have been included. $\langle P_{CN} \rangle$ for these reactions has been extracted by comparing experimental and theoretical ER excitation functions in the energy range $\sim$5%–35% above the potential barrier, where known effects of nuclear structure are insignificant.

**Results:** $\langle P_{CN} \rangle$ has been shown to vary with entrance channel mass asymmetry, $\eta$, (or charge product, $Z_p Z_t$), as well as with fissility of the CN, $\chi_{CN}$. No parameter has been found to be adequate as a single scaling variable to determine $\langle P_{CN} \rangle$. Approximate boundaries have been obtained from where $\langle P_{CN} \rangle$ starts deviating from unity.

**Conclusions:** This study quite clearly reveals the limits of applicability of the SM in interpreting experimental observables from fusion reactions involving two massive nuclei. Deviation of $\langle P_{CN} \rangle$ from unity marks the beginning of the domain of dynamical models of fusion. Availability of precise ER cross sections over a wider energy range for many more reactions is desired for accurate determination of $\langle P_{CN} \rangle$ and more insight into the dynamics of fusion in the heavy mass region.

## I. INTRODUCTION

Fusion is a process in which two nuclei merge with each other to produce a heavier nucleus. Currently, the heaviest man-made elements that could be studied in laboratories [1] have been synthesized using heavy-ion-induced complete fusion reactions. The two participating nuclei, after overcoming the potential barrier in the entrance channel, form a single entity, i.e., the compound nucleus (CN). The CN is equilibrated in all degrees of freedom and does not retain memories of the individual constituents of the entrance channel [2]. It cools off by emission of high energy statistical $\gamma$ rays, neutrons, light charged particles, and finally a cascade of low energy yrast $\gamma$ rays. The most certain experimental confirmation of fusion is the identification of the residual nucleus, i.e., the evaporation residue (ER). The other commonly used experimental method to study fusion is identification of one or more yrast $\gamma$ rays characteristic of a specific ER. This rather simple picture is sufficient to describe fusion reactions leading to light and medium-heavy CN. In heavier CN, another process, termed fission [3], competes with particle evaporation, in which the

CN splits itself (nearly) symmetrically into two halves under the influence of strong Coulomb repulsion. In still heavier systems, fission-like fragments are observed, which are created right after the entrance channel constituents overcome the potential barrier, bypassing formation of the CN. Production of cold ERs from fusion between two massive nuclei, thus, is a very complex process. The ER formation cross section is often decomposed over partial waves ($\ell$) and factorized as

$$\sigma_{ER}(E_{c.m.}) = \sum_{\ell=0}^{\infty} \sigma_{cap}(E_{c.m.}, \ell) P_{CN}(E_{c.m.}, \ell) P_{sur}(E^*, \ell). \quad (1)$$

Here $E_{c.m.}$ is the projectile energy in the center of mass (c.m.) frame, $E^*$ is the excitation energy of the CN and

$$\sigma_{cap}(E_{c.m.}) = \frac{\pi \hbar^2}{2\mu E_{c.m.}} \sum_{\ell=0}^{\infty} (2\ell + 1) T(E_{c.m.}, \ell) \quad (2)$$

is the capture cross section. $\frac{\hbar^2}{2\mu E_{c.m.}} (= \bar{\lambda}^2)$, $\mu$, and $T(E_{c.m.}, \ell)$ are reduced de Broglie wavelength, reduced mass in the entrance channel, and probability of the colliding nuclei to overcome the potential barrier in the entrance channel. $P_{CN}(E_{c.m.}, \ell)$ is the probability that the composite system will evolve from a configuration of two touching nuclei inside the fission saddle point and into a (nearly) spherical mononucleus, i.e., the CN. (This term is also called *fusion probability*, and denoted by $P_{fus}$

---
*subir@iuac.res.in
†Formerly with Physics Group, Variable Energy Cyclotron Centre, 1/AF Bidhan Nagar, Kolkata 700064, India.

by some authors.) The last factor in Eq. (1), i.e., $P_{sur}(E^*, \ell)$, is the probability that the CN will survive fission (also called fusion-fission or "true" fission by some authors) and yield a cold ER. According to Bohr's independence hypothesis, $P_{sur}(E^*, \ell)$ does not depend on the entrance channel.

Equation (1) may appear to suggest that ER formation involving two massive nuclei is a combination of three *independent* processes: (a) transition of the colliding nuclei over the potential barrier or capture, (b) CN formation or fusion, and (c) survival against fission. We must note here that such schematic factorization of $\sigma_{ER}$ into three terms is only approximate and often a matter of convenience, as the three phases of the reaction are connected with each other. An effort to formulate a "more physically correct" version of Eq. (1) was recently reported by Rowley and Grar [4]. Nevertheless, Eq. (1) can be fairly justified by noting the fact that the time scales are different for the three reaction stages, as was pointed out by Zagrebaev *et al.* [5]. Despite limitations, Eq. (1) has been used widely by theorists to model heavy ER formation in fusion reactions as well as by experimentalists to interpret measured cross sections.

For light and medium-heavy systems, both $P_{CN} \approx 1$ and $P_{sur} \approx 1$ and we can write $\sigma_{ER} \approx \sigma_{cap}$. For heavier systems, $P_{CN} \approx 1$ but $P_{sur} < 1$ and it decreases with increasing fissility of the CN. Here we can write $\sigma_{ER} \approx \sigma_{cap} \times P_{sur}$. (It may be mentioned here that the terms "capture" and "fusion" are often used interchangeably in literature, specifically for cases in which $P_{CN} \approx 1$. However, we make a clear distinction between these two terms in this article.) In very heavy systems, both $P_{CN} < 1$ and $P_{sur} < 1$. We must note that segregation of nuclear reactions leading to CN in medium-heavy, heavy, and very heavy mass regions is not unique and is rather arbitrary. Demarcating nuclear mass regions from where $P_{sur}$ and, particularly, $P_{CN}$ start deviating from unity is still a very formidable task both theoretically and experimentally.

Based on the preceding description, we may also write

$$\sigma_{cap} = \sigma_{fus} + \sigma_{NCNF}. \tag{3}$$

Here, $\sigma_{NCNF}$ is the cross section for fission-like processes which *do not* proceed via CN formation (i.e., non-compound-nucleus fission, NCNF). $\sigma_{NCNF}$ can be further subdivided into different classes of fission-like processes, e.g., (a) fast fission [6], (b) quasifission [7], and (c) pre-equilibrium fission [8]. However, these processes cannot be clearly distinguished experimentally and it would suffice to quantify all noncompound events taking place after capture by $\sigma_{NCNF}$ alone in the present work. $\sigma_{fus}$ is the fusion cross section and is the sum of cross sections of two distinct processes,

$$\sigma_{fus} = \sigma_{ER} + \sigma_{CNF}, \tag{4}$$

$\sigma_{CNF}$ being the cross section for fission which is one of the decay modes of the CN.

Fusion reactions that lead to formation of superheavy elements (SHE), can be of two broad classes: cold fusion (CN excitation energy $E^* \lesssim 15$ MeV, one or two neutron evaporation in the exit channel) and hot fusion ($E^* \gtrsim 30$ MeV, three or more neutron evaporation in the exit channel). Both

classes of reactions are characterized by $P_{CN} \ll 1$, which makes SHE synthesis in the laboratory extremely challenging. Such experiments are resource intensive and are carried out over a very long duration. Therefore, theoretical prediction of $\sigma_{ER}$ is of paramount importance to the experimentalists engaged in synthesizing SHE. Despite uncertainties and challenges, there is considerable consensus among theorists that the first and the last phases of the reactions, viz., capture and survival against fission, can be described theoretically with reasonable accuracy. One may adopt the coupled-channels approach for estimating $\sigma_{cap}$, which has been quite successful over a wide mass region. Survival of the excited CN against fission is usually treated within the framework of the SM. (We discuss the underlying uncertainties in calculating $\sigma_{cap}$ and $P_{sur}$ in Sec. IV.) Thus, the task of *accurate* prediction of $\sigma_{ER}$ boils down to how well one can determine $P_{CN}$.

Early theoretical investigations into the problem of fusion between two massive nuclei [9–11] suggested the need of an "extra push" energy to achieve complete fusion overcoming the dynamical suppression in the entrance channel. In this approach, it is assumed that the projectile and the target lose their individualities entirely after touching and the composite system is treated as a single strongly deformed mononucleus. This mononucleus evolves in the multidimensional space of deformations into a spherical CN or reseparates via NCNF. The distance between centers of the two nuclei, i.e., elongation, is assumed to be the most important degree of freedom. The "dinuclear system" (DNS) model [12–17], on the other hand, assumes that the nucleus-nucleus potential energy is diabatic and the colliding nuclei maintain their individual existence. Nucleon transfer between the two nuclei decides the evolution of the DNS. Zagrevbaev [18] proposed a model that is in between these two rather *extreme* approaches. Here, a certain number of "collectivized" nucleons are shared between the colliding nuclei. When all the nucleons belonging to both the nuclei are collectivized, the system evolves as the CN. The opposite, i.e., decollectivization of nucleons, leads to NCNF. Diaz-Torres [19,20] proposed a model based on the dynamical collective potential energy surface (PES). In this model, a gradual transition from the diabatic to the adiabatic PES results in formation of CN or NCNF from the initial contact configuration. Another approach to estimate $P_{CN}$ theoretically is the "fusion by diffusion" (FBD) model, proposed by Świątecki and collaborators [21–23]. Here, CN formation is described as diffusion over the multidimensional PES. Aritomo *et al.* [24,25] proposed a model which combined the coupled-channels approach for capture and a "fluctuation-dissipation model" for the subsequent dynamical evolution of the composite system. In this model, CNF and NCNF are separated by different Langevin trajectories on the PES. Very recently Kaur *et al.* [26] reported determination of $P_{CN}$ for a number of hot fusion reactions using the "dynamical cluster-decay model" (DCM). Despite a multitude of theoretical approaches, no single model to estimate $P_{CN}$ is predominant at this juncture.

Sahm *et al.* [27] proposed a simple parametrization of energy dependence of $P_{CN}$. Another approximate expression of $P_{CN}$ as a function of $E^*$ was reported by Zagrebaev *et al.* [5]. There also exist a number of systematics on $P_{CN}$ [28–32],

parametrized to be specifically applicable to either cold or hot fusion reactions.

Efforts have been made over the last three decades to *measure* $P_{CN}$ using different experimental probes. $P_{CN}$ values have been extracted for hot [33] and cold fusion [34] reactions by analyzing the shape of the measured fission fragment (FF) angular distributions. This method was first proposed by Back *et al.* [35], as a means to decompose the observed FF angular distribution into CNF and NCNF, and later followed by others [36]. Though the approach is quite straightforward, it is not entirely model independent. Some rather arbitrary assumptions on $\ell$ and the moment of inertia are inherent in the decomposition process. One may also determine $P_{CN}$ by analyzing FF mass and total kinetic energy (TKE) distributions [37,38]. This approach assumes that CNF yields symmetric mass distribution whereas NCNF leads to asymmetric mass split of the composite system. The assumption is only approximately true. There is strong evidence (e.g., Ref. [39]) that NCNF too can yield symmetric mass distribution. FF mass and angular distributions [40] have been used to estimate $P_{CN}$ for a number of systems.

We may add here that systematic investigations of NCNF, using FF angular distribution [41] and FF mass distribution [42] have also been reported recently. However, these studies focus on whether NCNF is present in a system rather than *quantification* of NCNF in the form of $P_{CN}$. Du Rietz *et al.* [43] have presented a detailed study of mass-angle distributions (MAD) for 42 reactions. The aim of this work has been to "map out the systematic dependence of NCNF characteristics as a function of the identity of the colliding nuclei" and provide "an empirical baseline" for NCNF instead of estimating $P_{CN}$ alone, which is an "integral of the dynamics."

CNF and NCNF often reveal overlapping experimental signatures which may lead to over or underestimation of $P_{CN}$ [32], if the same is extracted from fission-data. On the other hand, detection of ERs is the unambiguous signature of CN formation. A number of recent studies [44–47] focused on probing for the presence of NCNF from measured ER excitation functions. In this approach, $\sigma_{ER}$ is measured for a number of reactions with different $\eta$ ($= \frac{|A_p - A_t|}{A_p + A_t}$, $A_p$ and $A_t$ being mass number of projectile and target, respectively), leading to a specific CN. Measurements are carried out at $E^* \gtrsim 40$ MeV to ensure that all $\ell$ values are populated and $P_{CN}$ is independent of $E^*$. Reduced ER cross sections ($\tilde{\sigma}_{ER} = \frac{\sigma_{ER}}{\pi \tilde{\lambda}^2}$), plotted as a function of $E^*$ for all the reactions, reveal suppression of ER formation (also called *fusion hindrance*) for more symmetric systems. If one *assumes* that NCNF is negligible (i.e., $P_{CN} \simeq 1$) for the most asymmetric reaction, average CN formation probability ($\langle P_{CN} \rangle$) for any other reaction can be extracted by taking the ratio between $\sigma_{ER}$ of the two reactions at a suitable energy above the potential barrier. Another approach had been adopted, first by Sahm *et al.* [27] and later by others [48–51], in which measured $\sigma_{ER}$ is compared against calculated $\sigma_{ER}$ to obtain $\langle P_{CN} \rangle$ for a given system. Recently, Sagaidak [32] reported such a calculation for a number of reactions. In this article, we follow the latter approach to work out a systematics of $P_{CN}$ using ER excitation function data available in the literature.

Most of the earlier works on $P_{CN}$ are concerned with systems in very-heavy and superheavy mass regions, where $\sigma_{ER}$ is a tiny fraction of $\sigma_{cap}$. Very little information is available on $P_{CN}$ in the heavy mass region, which is the focus of the present work. We are concerned about fusion between massive nuclei with mass of the composite system ($A_{CN}$) in the range of 170–220, where $\sigma_{ER}$ competes with both $\sigma_{CNF}$ and $\sigma_{NCNF}$.

The article is organized as follows. A general introduction and survey of existing work has been presented in this section. Section II describes the methodology adopted to determine $P_{CN}$ in this work. Results of our calculation are presented in Sec. III followed by a discussion in Sec. IV. We conclude in Sec. V.

## II. METHODOLOGY OF CALCULATION

### A. Average fusion probability

It follows from the work of Sahm *et al.* [27] that angular-momentum-averaged fusion probability for a given reaction can be defined as

$$\langle P_{CN} \rangle = \frac{\sigma_{ER}}{\sigma_{ER}^{max}}. \quad (5)$$

The numerator can be obtained from measurement and the denominator corresponds to the upper limit of the ER cross section. Needless to say, the ratio has to be taken at the same $E^*$ for both the numerator and the denominator (or, more generally, in the region where $P_{CN}$ has very weak dependence on $E^*$). $\sigma_{ER}^{max}$ can be obtained from the SM, which *inherently* assumes that $P_{CN} = 1$.

While comparing $\sigma_{ER}^{max}$ with $\sigma_{ER}$ for a particular system, three possibilities may arise: (a) the SM calculation reproduces measured ER excitation function, (b) the experimental ER excitation function is underestimated by the SM calculation, and (c) the SM calculation overestimates the measured ER excitation function. For case (a), $\langle P_{CN} \rangle$ is obviously 1. For case (b), $\langle P_{CN} \rangle$ is *assumed* to be 1, as probability cannot be more than 1 numerically. The enhanced $\sigma_{ER}$, with respect to the SM prediction, can be explained by invoking dissipation in the fission (i.e., CNF) process, as had been done in Ref. [52]. The third possibility, stated in (c) above, is the manifestation of reduction in average CN formation probability. $\langle P_{CN} \rangle$ is determined, in this case, by *scaling down* the calculated ER excitation function onto the experimental ER excitation function. In other words, the scaling down factor is taken as the $\langle P_{CN} \rangle$.

### B. Capture cross section

To obtain $\sigma_{ER}^{max}$, we have proceeded as follows. First we have calculated $\sigma_{cap}$ using the coupled-channels code CCFULL [53]. The Woods-Saxon parametrization of the Akyüz-Winther potential has been used for the three ingredients of the nuclear potential used in CCFULL: the depth $V_0$, the radius $r_0$, and the diffuseness parameter a. Proper rotational and vibrational couplings to the target and the projectile have been taken into account. For odd-mass projectile and/or target, the energy of the first excited state has been taken from the level scheme and the corresponding deformation has been taken

from standard tables. To ensure weak dependence of $P_{CN}$ on $E^*$, we have focused in the range of $E_{c.m.}$ typically $\sim 5\%$ to $\sim 35\%$ above the potential barrier, where known effects of static deformation, inelastic excitations of the participating nuclei, and their shell structures may not be significant. Also, this range represents the energy and angular momenta that are usually involved in experiments to synthesize SHE. The range of $E_{c.m.}$, chosen here, corresponds to $E^*$ in the range $\sim 40$–60 MeV for most of the reactions considered in this article. We have compared calculated $\sigma_{cap}$ with data for 38 reactions and found reasonably good agreement in the region of our interest. We have found only one major exception, where CCFULL does not reproduce experimental $\sigma_{cap}$. (We look into this point further in Sec. IV.) For the systems with no measured $\sigma_{cap}$ available in the literature, we have relied upon the same scheme of parametrization. The partial cross sections $\sigma_\ell$, at each energy point for a given system, which are generated by CCFULL have then been fed as the input of an SM [54] code to obtain $\sigma_{ER}^{max}$.

### C. Statistical model calculation

In the SM calculation, we have considered emission of light particles ($\alpha$, $p$, and $n$), giant dipole resonance (GDR) $\gamma$ rays, and fission as the possible decay channels of the CN. Decay widths of light particles and GDR $\gamma$ emission have been obtained from the Weisskopf formula, as given in Ref. [55]. Experimental nuclear masses have been used to calculate particle separation energies in the particle decay width calculation. Fission width has been taken from the transition-state model of Bohr and Wheeler, which is given as [56]

$$\Gamma_{BW} = \frac{1}{2\pi\rho_g(E_i)} \int_0^{E_i - B_f} \rho_s(E_i - B_f - \epsilon)d\epsilon, \qquad (6)$$

where $\rho_g$ and $\rho_s$ are the level densities at the ground state and the saddle configurations, respectively, $E_i$ is the initial excitation energy, and $B_f$ is the fission barrier. We further multiply $\Gamma_{BW}$ by the phase-space factor $\frac{\hbar\omega_g}{T}$, which takes into account the collective degrees of freedom in the ground state [57]. Here $\omega_g$ stands for the frequency of a harmonic oscillator potential having the same curvature as the nuclear potential at the ground state, while $T$ is the nuclear temperature. The fate of the CN is decided by the competition between the different decay widths.
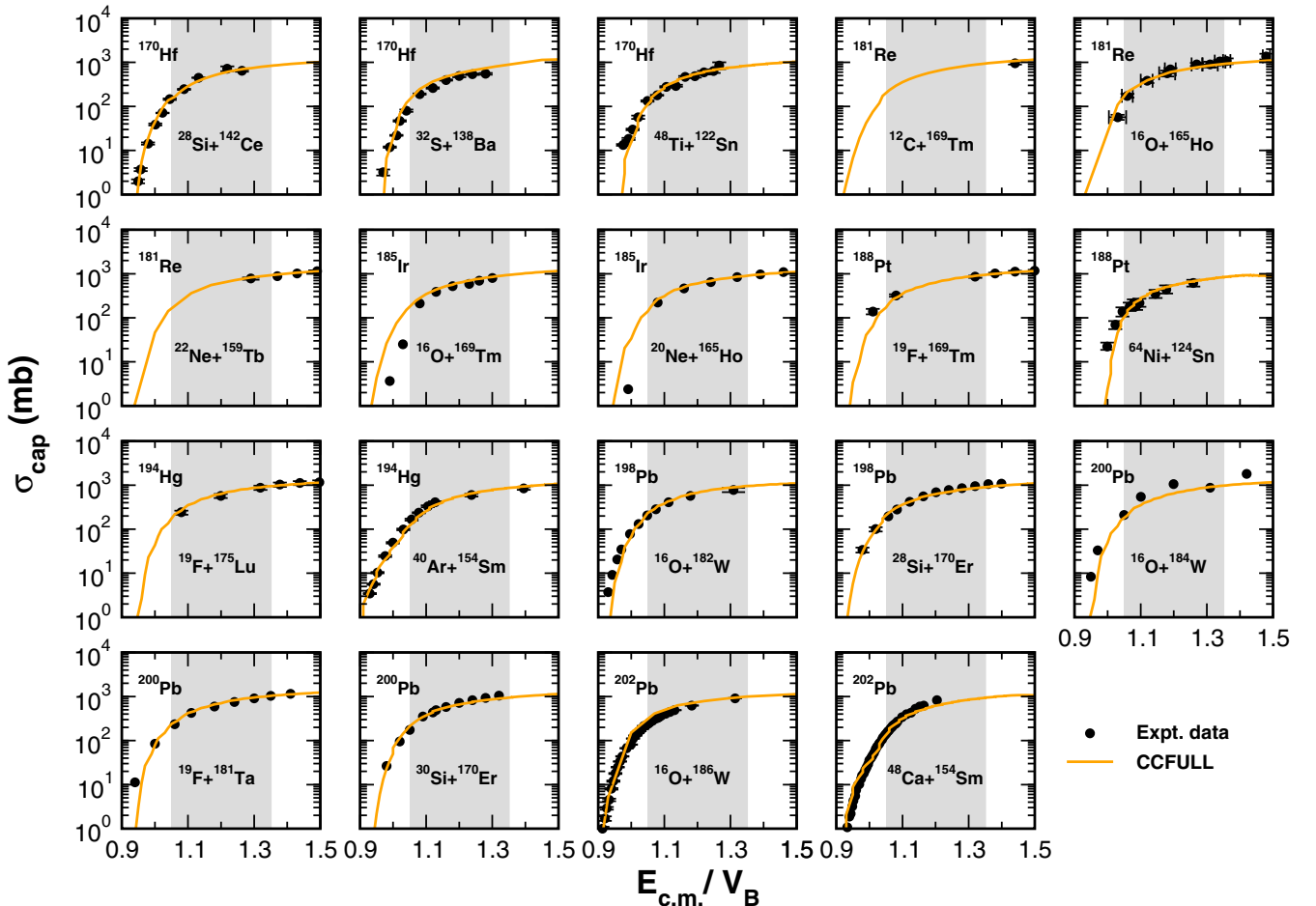


FIG. 1. (Color online) Capture cross sections as a function of $\frac{E_{c.m.}}{V_B}$ for 19 reactions leading to CN $^{170}$Hf, $^{181}$Re, $^{185}$Ir, $^{188}$Pt, $^{194}$Hg, $^{198}$Pb, $^{200}$Pb, and $^{202}$Pb. The solid line in each panel represents the result of the CCFULL calculation. The shaded region denotes range of $E_{c.m.}$ from 5% to 35% above the $V_B$, the focus of the present work. See text for details.

Intensity of different decay modes is decided by the nuclear level density, which is defined as [58]

$$\rho(E,\ell) = \frac{2\ell + 1}{24}\left(\frac{\hbar^2}{2\mathfrak{I}}\right)^{\frac{3}{2}} \sqrt{a}\,\frac{\exp(2\sqrt{aE^*})}{E^{*2}}, \qquad (7)$$

where $\mathfrak{I}$ is the moment of inertia. The level density parameter, $a$, has been taken from the work of Ignatyuk *et al.* [59] and is given as follows:

$$a(E^*) = \tilde{a}\left(1 + \frac{1 - \exp\left(-\frac{E^*}{E_\mathrm{D}}\right)}{E^*}\delta W\right). \qquad (8)$$

Here, $\tilde{a}$ is the asymptotic value to which the level density parameter approaches with increasing $E^*$ of the CN. $\tilde{a}$ depends upon the nuclear mass and the shape in a fashion similar to that of the liquid drop model of mass [60]. $E_\mathrm{D}$ accounts for the rate at which the shell effect melts away with an increase of $E^*$. A value of 18.5 MeV has been used for $E_\mathrm{D}$ which was obtained from analysis of $s$-wave neutron resonances [60]. The shell correction term $\delta W$ is given as the difference between the experimental and liquid drop model (LDM) masses, i.e., $\delta W = M_\mathrm{exp} - M_\mathrm{LDM}$.

The finite-range liquid drop model (FRLDM) potential has been used to calculate fission barriers [61]. Following the suggestion of Aritomo [62], an $E^*$-dependent shell correction has been applied to the FRLDM fission barriers. The parametrized form of the shell-corrected fission barrier for a CN with angular momentum $\ell$ is given as

$$B_\mathrm{f}(\ell, E^*) = B_\mathrm{f}^\mathrm{LDM}(\ell) - f_\ell \delta W \exp\left(-\frac{E^*}{E_\mathrm{D}}\right), \qquad (9)$$

where $B_\mathrm{f}^\mathrm{LDM}(\ell)$ is the fission barrier at angular momentum $\ell$ from the FRLDM potential. The scaling factor $f_\ell$ ensures that shell correction vanishes when the saddle and ground state configurations become very close at large angular momentum [63]. A simple ansatz, $f_\ell = \frac{B_\mathrm{f}^\mathrm{LDM}(\ell)}{B_\mathrm{f}^\mathrm{LDM}(0)}$, has been used for this purpose here.

We have calculated ER excitation functions for 52 reactions using the model described above. No attempt has been made to adjust any of the several parameters for individual cases. Calculation for each reaction has been performed with sufficiently large ensemble to ensure that the statistical uncertainties in $\sigma_\mathrm{ER}^\mathrm{max}$ do not exceed 2%.
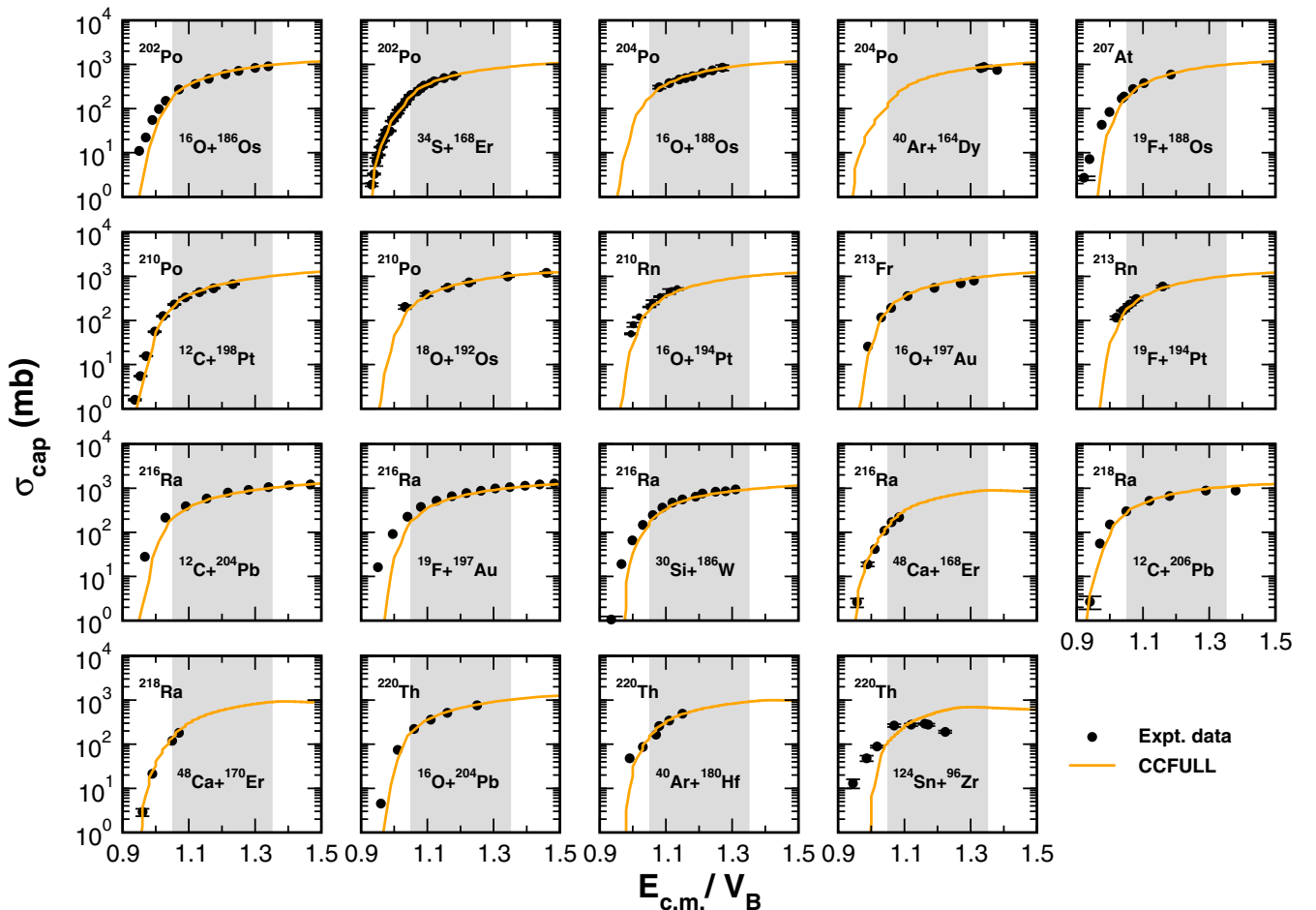


FIG. 2. (Color online) Capture cross sections as a function of $\frac{E_\mathrm{c.m.}}{V_\mathrm{B}}$ for 19 reactions leading to CN $^{202}$Po, $^{204}$Po, $^{207}$At, $^{210}$Po, $^{210}$Rn, $^{213}$Fr, $^{216}$Ra, $^{218}$Ra, and $^{220}$Th. The solid line in each panel represents the result of the CCFULL calculation. The shaded region denotes range of $E_\mathrm{c.m.}$ from 5% to 35% above the $V_\mathrm{B}$, the focus of the present work. See text for details.

## III. RESULTS

Results from CCFULL, i.e., $\sigma_{\text{cap}}$ as a function of $\frac{E_{\text{c.m.}}}{V_{\text{B}}}$, for 38 reactions are shown in Figs. 1 and 2. Measured ER excitation functions for 52 reactions along with SM predictions are shown in Figs. 3–5. Results of our calculation for all the reactions, with $A_{\text{CN}}$ in the range 170–220, are listed in Table I. We have included only those nuclei for which $\sigma_{\text{ER}}$ are available with at least two entrance channels.

Out of 52 reactions, only a single reaction, viz. $^{16}$O + $^{184}$W [52] has been found to exhibit *dissipation* in fission (Fig. 3). However, $\sigma_{\text{ER}}$ for the same reaction, as reported in Ref. [80], have been reproduced very well by our SM calculation. We note that calculated ER excitation function exceeds measured ER excitation function for the reaction $^{32}$S + $^{138}$Ba by ~15% (Fig. 3). We also notice that the calculated capture excitation function for this system exceeds the measured capture excitation function by nearly the same factor (Fig. 1). Hence, we have assigned $\langle P_{\text{CN}} \rangle = 1$ for this reaction.

Table I lists CN fissility ($\chi_{\text{CN}}$), charge product in the entrance channel ($Z_{\text{p}}Z_{\text{t}}$), effective entrance channel fissility ($\chi_{\text{eff}}$), $\eta$ and $\eta_{\text{BG}}$ along with $\langle P_{\text{CN}} \rangle$ for each reaction. Here,

$\eta_{\text{BG}}$ is the Businaro-Gallone critical mass asymmetry [121]. $\chi_{\text{CN}}$ is defined as [11]

$$\chi_{\text{CN}} = \frac{Z^2}{A} \bigg/ \left(\frac{Z^2}{A}\right)_{\text{crit}}, \tag{10}$$

where $Z$ and $A$ are the atomic and mass numbers of the CN, respectively. The denominator is taken as

$$\left(\frac{Z^2}{A}\right)_{\text{crit}} = 50.883(1 - 1.7826\,I^2), \tag{11}$$

where $I = \frac{(A-2Z)}{A}$ is the relative neutron excess of the CN. $\chi_{\text{eff}}$ is defined as [11]

$$\chi_{\text{eff}} = \frac{4Z_1 Z_2}{\left[A_1^{\frac{1}{3}} A_2^{\frac{1}{3}} \left(A_1^{\frac{1}{3}} + A_2^{\frac{1}{3}}\right)\right]} \bigg/ \left(\frac{Z^2}{A}\right)_{\text{crit}}. \tag{12}$$

By scrutinizing Table I, one can make the following general conclusions:

(i) $\langle P_{\text{CN}} \rangle$ decreases with increasing $A_{\text{CN}}$ and/or $\chi_{\text{CN}}$.

(ii) For a given CN, $\langle P_{\text{CN}} \rangle$ decreases with increasing $Z_{\text{p}}Z_{\text{t}}$ and decreasing $\eta$.
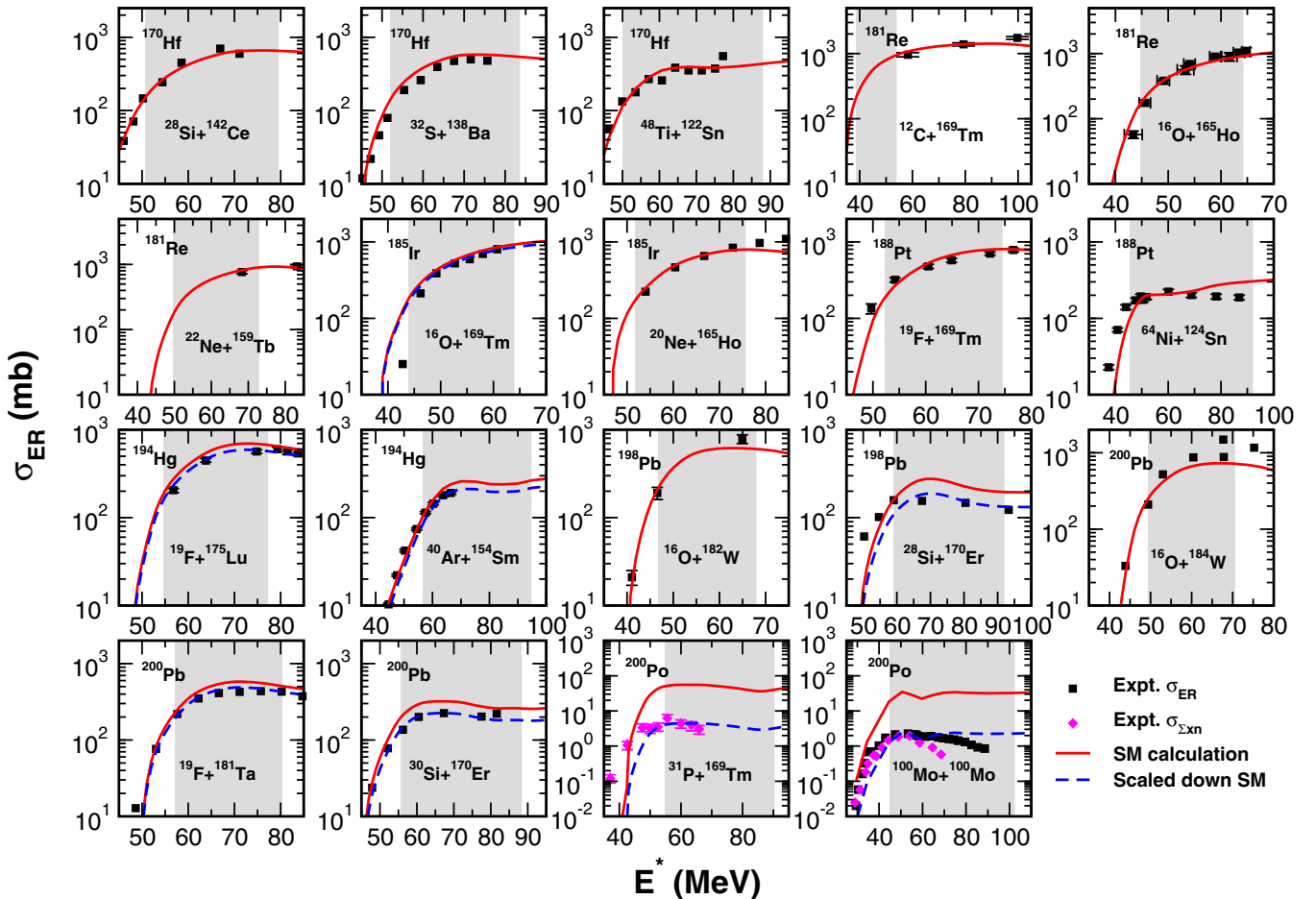


FIG. 3. (Color online) ER cross sections (or $\sigma_{\Sigma xn}$) as a function of $E^*$ for 19 reactions leading to CN $^{170}$Hf, $^{181}$Re, $^{185}$Ir, $^{188}$Pt, $^{194}$Hg, $^{198}$Pb, $^{200}$Pb, and $^{200}$Po. The solid line in each panel represents the result of the SM calculation, whereas the dashed line stands for the scaled-down SM calculation to match experimental data. The shaded region denotes the range of $E^*$ corresponding to $\frac{E_{\text{c.m.}}}{V_{\text{B}}}$ from 5% to 35% above the $V_{\text{B}}$. See text for details.

FIG. 4. (Color online) ER cross sections (or $\sigma_{\Sigma xn}$) as a function of $E^*$ for 20 reactions leading to CN $^{202}$Pb, $^{202}$Po, $^{204}$Po, $^{207}$At, $^{210}$Po, $^{210}$Rn, $^{212}$Rn, and $^{213}$Fr. The solid line in each panel represents the result of the SM calculation, whereas the dashed line stands for the scaled-down SM calculation to match experimental data. The shaded region denotes the range of $E^*$ corresponding to $\frac{E_{\text{c.m.}}}{V_B}$ from 5% to 35% above the $V_B$. See text for details.
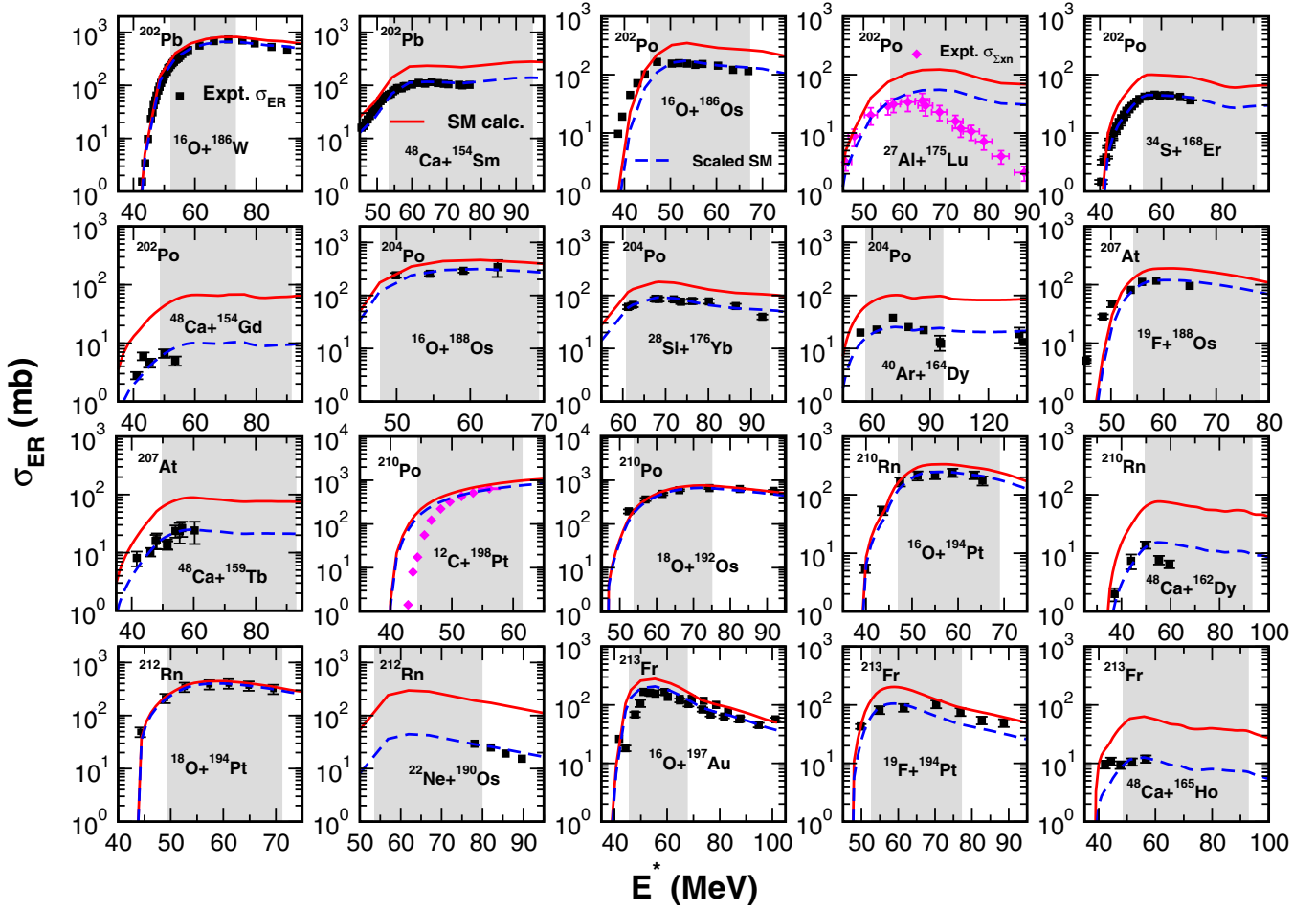
(iii) About a quarter of the systems exhibit different rates of variation of $\langle P_{\text{CN}} \rangle$ as a function of $\eta$ or $Z_p Z_t$, compared to the rest.

(iv) For five reactions, $\sigma_{\text{ER}}$ are not available. We have used $\sigma_{\Sigma xn}$ instead to determine $\langle P_{\text{CN}} \rangle$. If $\sigma_{\text{ER}}$ are measured and used in determining $\langle P_{\text{CN}} \rangle$, the same are expected to go up compared to the values listed in Table I.

(v) For six reactions, (i) $^{16}$O + $^{186}$Os, (ii) $^{48}$Ca + $^{154}$Gd, (iii) $^{48}$Ca + $^{162}$Dy, (iv) $^{22}$Ne + $^{190}$Os, (v) $^{22}$Ne + $^{196}$Pt, and (vi) $^{40}$Ar + $^{180}$Hf, $\langle P_{\text{CN}} \rangle$ is much lower than *expected* from the general trends, even though $\sigma_{\text{ER}}$ have been used to determine the same.

To understand possible variation of $\langle P_{\text{CN}} \rangle$ with different reaction parameters and to look for any underlying pattern that may emerge from the data set, we have plotted $\langle P_{\text{CN}} \rangle$ as a function of $Z_p Z_t$, $\eta$, $\chi_{\text{eff}}$, and $\chi_{\text{CN}}$ in Fig. 6. We notice that no new pattern emerges apart from the general observations already listed. It is obvious that $\langle P_{\text{CN}} \rangle$ is a multivalued function of each of the four variables plotted along the horizontal axes of the four panels in Fig. 6. Nevertheless, we highlight the following:

(i) The systems $^{64}$Ni + $^{124}$Sn and $^{48}$Ca + $^{172}$Yb have the same $Z_p Z_t$, but $\langle P_{\text{CN}} \rangle$ for the two reactions differ widely, 1.00 and 0.03, respectively.

(ii) Though $\chi_{\text{eff}}$ for $^{20}$Ne + $^{165}$Ho (0.454) and $^{19}$F + $^{197}$Au (0.452) are quite similar, $\langle P_{\text{CN}} \rangle$ for the two reactions, 1.00 and 0.37, respectively, are very dissimilar.

(iii) Despite having nearly equal $\eta$, 0.823 and 0.824, respectively, $\langle P_{\text{CN}} \rangle$ for the systems $^{16}$O + $^{165}$Ho (1.00) and $^{19}$F + $^{197}$Au (0.37) are quite different.

We can, therefore, conclude that no parameter is adequate as a single scaling variable to determine $\langle P_{\text{CN}} \rangle$. A similar conclusion has recently been drawn by Yanez *et al.* [33].

We have next plotted $\langle P_{\text{CN}} \rangle$ (Fig. 7) as a function of two variables: (a) one for the entrance channel ($Z_p Z_t$ or $\eta$) and (b) one for the composite system ($\chi_{\text{CN}}$). The surfaces have been *constructed* by interpolation and extrapolation based on the data points presented in Table I. We clearly state here that "accuracy" and "uniqueness" of the surfaces can not be fully ensured because of (a) availability of very few (i.e., 52) data points and (b) nonuniform distribution of the population in the respective planes defined by $Z_p Z_t - \chi_{\text{CN}}$
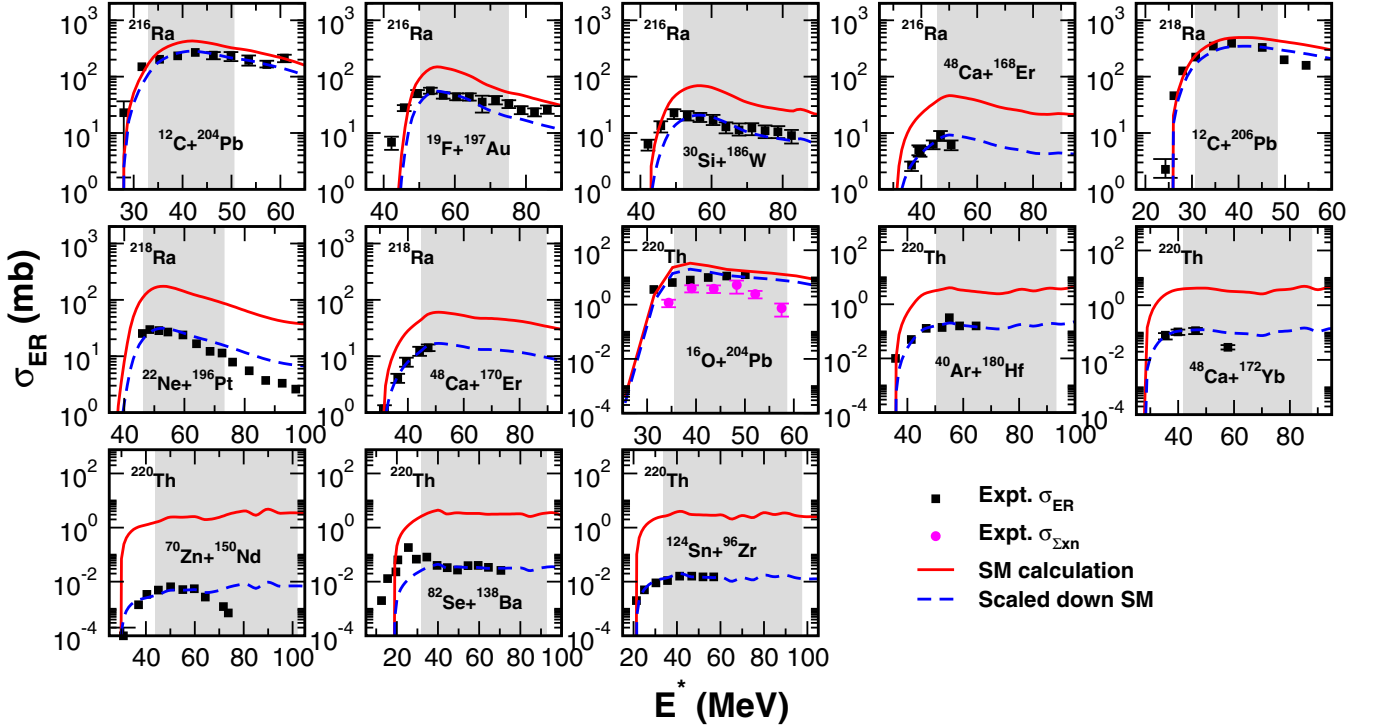
FIG. 5. (Color online) ER cross sections (or $\sigma_{\Sigma xn}$) as a function of $E^*$ for 13 reactions leading to CN $^{216}$Ra, $^{218}$Ra, and $^{220}$Th. The solid line in each panel represents the result of the SM calculation, whereas the dashed line stands for the scaled-down SM calculation to match experimental data. The shaded region denotes the range of $E^*$ corresponding to $\frac{E_{\mathrm{c.m.}}}{V_{\mathrm{B}}}$ from 5% to 35% above the $V_{\mathrm{B}}$. See text for details.

and $\eta-\chi_{\mathrm{CN}}$. Consequently, large uncertainties may be present in the regions with low population density. Availability of more data points (i.e., measured ER excitation functions for many more systems) will aid in reducing these uncertainties significantly.

However, one may quite convincingly identify approximate boundaries from where $\langle P_{\mathrm{CN}} \rangle$ starts deviating from unity. The boundaries are shown in Fig. 8. The straight lines, which are shown in the two panels to divide the regions with $\langle P_{\mathrm{CN}} \rangle = 1$ and $\langle P_{\mathrm{CN}} \rangle < 1$, are defined by the equations

$$\chi_{\mathrm{CN}} = 0.727 - 3.9 \times 10^{-5} Z_p Z_t \tag{13}$$

in panel (a) and

$$\chi_{\mathrm{CN}} = 0.062\eta + 0.651 \tag{14}$$

in panel (b), respectively.

We may recall here that $\langle P_{\mathrm{CN}} \rangle < 1$ implies presence of NCNF, which cannot be accounted for in the SM. In other words, the straight lines defined by Eqs. (13) and (14) show the approximate limits of applicability of the SM in interpreting experimental observables from fusion reactions involving massive nuclei. Systems located above these lines in both panels of Fig. 8 should instead be analyzed using a dynamical model of fusion.

## IV. DISCUSSION

We argued that $\langle P_{\mathrm{CN}} \rangle$ determined from FF mass and angular distribution data may not be unambiguous as CNF and NCNF both have overlapping experimental signatures. ER formation,

on the other hand, is the unambiguous evidence of CN formation or fusion. However, $\langle P_{\mathrm{CN}} \rangle$ values extracted from ER excitation function data may also include large uncertainties. There are two broad methods to extract $\langle P_{\mathrm{CN}} \rangle$ from $\sigma_{\mathrm{ER}}$. The method followed in Refs. [32,46,47] assumes that $\langle P_{\mathrm{CN}} \rangle \simeq 1$ for the most asymmetric reaction. This assumption is questionable as it does not consider possible variation of $\langle P_{\mathrm{CN}} \rangle$ with increasing $A_{\mathrm{CN}}$ (or $\chi_{\mathrm{CN}}$). The other method, proposed by Sahm *et al.* [27] and followed in this article relies heavily on model calculations.

A major source of uncertainty in calculated $\sigma_{\mathrm{ER}}$ is the $\sigma_{\mathrm{cap}}$. Loveland [122] pointed out that uncertainties in calculated $\sigma_{\mathrm{cap}}$ may be as high as an order of magnitude in the SHE mass region. We emphasize here that measured $\sigma_{\mathrm{cap}}$ are available for many systems in the mass region of our interest. We found reasonably good agreement between measured $\sigma_{\mathrm{cap}}$ and CCFULL predictions for most of the cases for which data were available in the literature. Woods-Saxon parameterization of the Akyüz-Winther potential could reproduce data points quite well in the energy regime of our interest. This is evident from the plots shown in Figs. 1 and 2. A notable exception is the reaction $^{124}$Sn + $^{96}$Zr [120]. The authors of Ref. [120] reproduced measured $\sigma_{\mathrm{cap}}$ with the DNS model calculation and showed that the coupled-channels calculation failed to explain their data. However, for consistency, we have used same prescription for the potential parameters in all 52 cases. We must mention here that the SM calculation, initiated with CCFULL $\sigma_\ell$-distribution, has reproduced the shape of the ER excitation function for $^{124}$Sn + $^{96}$Zr quite well. We conclude here that the uncertainties, caused by calculated $\sigma_{\mathrm{cap}}$

TABLE I. Reactions for which $\langle P_{CN} \rangle$ have been determined in this article. Potential barriers (in the c.m. frame), $V_B$, are calculated using the prescription given in Ref. [64]. Experimental masses to calculate $Q$ values are taken from Ref. [65]. References for measured ER, fission, and capture excitation functions (whichever are available) are given in the last column.

| CN | $\chi_{CN}$ | $\eta_{BG}$ | System | $V_B$ (MeV) | $Q$ value (MeV) | $Z_p Z_t$ | $\chi_{eff}$ | $\eta$ | $\langle P_{CN} \rangle$ | Ref. |
|---|---|---|---|---|---|---|---|---|---|---|
| $^{170}_{72}\text{Hf}_{98}$ | 0.625 | 0.783 | $^{28}_{14}\text{Si} + ^{142}_{58}\text{Ce}$ | 95.70 | −49.772 | 812 | 0.509 | 0.671 | 1.00 | [66] |
| | | | $^{32}_{16}\text{S} + ^{138}_{56}\text{Ba}$ | 104.79 | −58.024 | 896 | 0.537 | 0.624 | 1.00 | [66] |
| | | | $^{48}_{22}\text{Ti} + ^{122}_{50}\text{Sn}$ | 125.91 | −82.179 | 1100 | 0.583 | 0.435 | 1.00 | [66] |
| $^{181}_{75}\text{Re}_{106}$ | 0.644 | 0.799 | $^{12}_{6}\text{C} + ^{169}_{69}\text{Tm}$ | 50.72 | −14.755 | 414 | 0.347 | 0.867 | 1.00 | [67] |
| | | | $^{16}_{8}\text{O} + ^{165}_{67}\text{Ho}$ | 64.58 | −23.114 | 536 | 0.402 | 0.823 | 1.00 | [68,69] |
| | | | $^{22}_{10}\text{Ne} + ^{159}_{65}\text{Tb}$ | 76.84 | −31.035 | 650 | 0.432 | 0.757 | 1.00 | [67] |
| $^{185}_{77}\text{Ir}_{103}$ | 0.663 | 0.813 | $^{16}_{8}\text{O} + ^{169}_{69}\text{Tm}$ | 66.25 | −25.677 | 552 | 0.407 | 0.827 | 0.92 | [70] |
| | | | $^{20}_{10}\text{Ne} + ^{165}_{67}\text{Ho}$ | 79.34 | −31.605 | 670 | 0.454 | 0.784 | 1.00 | [71] |
| $^{188}_{78}\text{Pt}_{110}$ | 0.671 | 0.818 | $^{19}_{9}\text{F} + ^{169}_{69}\text{Tm}$ | 73.56 | −24.934 | 621 | 0.426 | 0.798 | 1.00 | [72] |
| | | | $^{64}_{28}\text{Ni} + ^{124}_{50}\text{Sn}$ | 155.08 | −117.504 | 1400 | 0.647 | 0.319 | 1.00 | [73,74] |
| $^{194}_{80}\text{Hg}_{114}$ | 0.686 | 0.828 | $^{19}_{9}\text{F} + ^{175}_{71}\text{Lu}$ | 75.26 | −24.471 | 639 | 0.431 | 0.804 | 0.85 | [75,76] |
| | | | $^{40}_{18}\text{Ar} + ^{154}_{62}\text{Sm}$ | 125.76 | −75.310 | 1116 | 0.577 | 0.588 | 0.82 | [77,78] |
| $^{198}_{82}\text{Pb}_{116}$ | 0.704 | 0.840 | $^{16}_{8}\text{O} + ^{182}_{74}\text{W}$ | 70.18 | −26.935 | 592 | 0.420 | 0.838 | 1.00 | [79,80] |
| | | | $^{28}_{14}\text{Si} + ^{170}_{68}\text{Er}$ | 109.13 | −55.552 | 952 | 0.548 | 0.717 | 0.68 | [81,82] |
| $^{200}_{82}\text{Pb}_{118}$ | 0.701 | 0.838 | $^{16}_{8}\text{O} + ^{184}_{74}\text{W}$ | 70.06 | −24.194 | 592 | 0.420 | 0.840 | 1.00 | [52,80,83] |
| | | | $^{19}_{9}\text{F} + ^{181}_{73}\text{Ta}$ | 76.96 | −23.678 | 657 | 0.436 | 0.810 | 0.84 | [72,84] |
| | | | $^{30}_{14}\text{Si} + ^{170}_{68}\text{Er}$ | 108.48 | −58.292 | 952 | 0.534 | 0.700 | 0.70 | [84] |
| $^{200}_{84}\text{Po}_{116}$ | 0.727 | 0.852 | $^{31}_{15}\text{P} + ^{169}_{69}\text{Tm}$ | 117.71 | −68.762 | 1035 | 0.566 | 0.690 | 0.08[a] | [85] |
| | | | $^{100}_{42}\text{Mo} + ^{100}_{42}\text{Mo}$ | 190.76 | −155.425 | 1764 | 0.727 | 0.000 | 0.07 | [50,86] |
| $^{202}_{82}\text{Pb}_{120}$ | 0.698 | 0.836 | $^{16}_{8}\text{O} + ^{186}_{74}\text{W}$ | 69.93 | −21.308 | 592 | 0.420 | 0.842 | 0.81 | [46,79,87,88] |
| | | | $^{48}_{20}\text{Ca} + ^{154}_{62}\text{Sm}$ | 137.27 | −90.739 | 1240 | 0.594 | 0.525 | 0.50 | [46,89] |
| $^{202}_{84}\text{Po}_{118}$ | 0.723 | 0.851 | $^{16}_{8}\text{O} + ^{186}_{76}\text{Os}$ | 71.82 | −29.815 | 608 | 0.425 | 0.842 | 0.50 | [90] |
| | | | $^{27}_{13}\text{Al} + ^{175}_{71}\text{Lu}$ | 105.65 | −54.440 | 923 | 0.530 | 0.733 | 0.45[a] | [85] |
| | | | $^{34}_{16}\text{S} + ^{168}_{68}\text{Er}$ | 122.83 | −74.998 | 1088 | 0.575 | 0.663 | 0.45 | [91,92] |
| | | | $^{48}_{20}\text{Ca} + ^{154}_{64}\text{Gd}$ | 141.70 | −100.006 | 1280 | 0.605 | 0.525 | 0.15 | [93] |
| $^{204}_{84}\text{Po}_{120}$ | 0.720 | 0.849 | $^{16}_{8}\text{O} + ^{188}_{76}\text{Os}$ | 71.69 | −27.536 | 608 | 0.425 | 0.843 | 0.68 | [94,95] |
| | | | $^{28}_{14}\text{Si} + ^{176}_{70}\text{Yb}$ | 111.73 | −56.642 | 980 | 0.555 | 0.725 | 0.51 | [96] |
| | | | $^{40}_{18}\text{Ar} + ^{164}_{66}\text{Dy}$ | 132.61 | −82.666 | 1188 | 0.594 | 0.608 | 0.25 | [97–99] |
| $^{207}_{85}\text{At}_{122}$ | 0.727 | 0.853 | $^{19}_{9}\text{F} + ^{188}_{76}\text{Os}$ | 79.62 | −29.400 | 684 | 0.444 | 0.816 | 0.63 | [100] |
| | | | $^{48}_{20}\text{Ca} + ^{159}_{65}\text{Tb}$ | 143.24 | −100.530 | 1300 | 0.608 | 0.536 | 0.28 | [93] |
| $^{210}_{84}\text{Po}_{126}$ | 0.711 | 0.844 | $^{12}_{6}\text{C} + ^{198}_{78}\text{Pt}$ | 55.82 | −13.953 | 468 | 0.366 | 0.886 | 0.78[a] | [101,102] |
| | | | $^{18}_{8}\text{O} + ^{192}_{76}\text{Os}$ | 70.82 | −20.714 | 608 | 0.406 | 0.829 | 0.88 | [72] |
| $^{210}_{86}\text{Rn}_{124}$ | 0.735 | 0.857 | $^{16}_{8}\text{O} + ^{194}_{78}\text{Pt}$ | 73.19 | −29.895 | 624 | 0.430 | 0.848 | 0.74 | [103,104] |
| | | | $^{48}_{20}\text{Ca} + ^{162}_{66}\text{Dy}$ | 145.04 | −102.800 | 1320 | 0.612 | 0.543 | 0.20 | [93] |
| $^{212}_{86}\text{Rn}_{126}$ | 0.732 | 0.855 | $^{18}_{8}\text{O} + ^{194}_{78}\text{Pt}$ | 72.56 | −26.886 | 624 | 0.411 | 0.830 | 0.90 | [105] |
| | | | $^{22}_{10}\text{Ne} + ^{190}_{76}\text{Os}$ | 87.31 | −38.075 | 760 | 0.463 | 0.792 | 0.15 | [106] |
| $^{213}_{87}\text{Fr}_{126}$ | 0.743 | 0.861 | $^{16}_{8}\text{O} + ^{197}_{79}\text{Au}$ | 73.94 | −32.325 | 632 | 0.432 | 0.850 | 0.60 | [107–110] |
| | | | $^{19}_{9}\text{F} + ^{194}_{78}\text{Pt}$ | 81.29 | −32.697 | 702 | 0.449 | 0.822 | 0.52 | [63,111] |
| | | | $^{48}_{20}\text{Ca} + ^{165}_{67}\text{Ho}$ | 146.84 | −105.570 | 1340 | 0.616 | 0.549 | 0.20 | [93] |
| $^{216}_{88}\text{Ra}_{128}$ | 0.750 | 0.865 | $^{12}_{6}\text{C} + ^{204}_{82}\text{Pb}$ | 58.38 | −28.401 | 492 | 0.374 | 0.889 | 0.66 | [112] |
| | | | $^{19}_{9}\text{F} + ^{197}_{79}\text{Au}$ | 82.13 | −35.920 | 711 | 0.452 | 0.824 | 0.37 | [112] |
| | | | $^{30}_{14}\text{Si} + ^{186}_{74}\text{W}$ | 116.40 | −70.235 | 1036 | 0.555 | 0.722 | 0.30 | [112] |
| | | | $^{48}_{20}\text{Ca} + ^{168}_{68}\text{Er}$ | 148.63 | −110.507 | 1360 | 0.620 | 0.556 | 0.20 | [113] |
| $^{218}_{88}\text{Ra}_{130}$ | 0.748 | 0.863 | $^{12}_{6}\text{C} + ^{206}_{82}\text{Pb}$ | 58.28 | −30.436 | 492 | 0.374 | 0.890 | 0.70 | [113] |
| | | | $^{22}_{10}\text{Ne} + ^{196}_{78}\text{Pt}$ | 89.15 | −47.323 | 780 | 0.469 | 0.798 | 0.18 | [114] |
| | | | $^{48}_{20}\text{Ca} + ^{170}_{68}\text{Er}$ | 148.37 | −110.985 | 1360 | 0.620 | 0.560 | 0.28 | [113] |

TABLE I. (*Continued.*)

| CN | $\chi_{CN}$ | $\eta_{BG}$ | System | $V_B$ (MeV) | $Q$ value (MeV) | $Z_p Z_t$ | $\chi_{eff}$ | $\eta$ | $\langle P_{CN} \rangle$ | Ref. |
|---|---|---|---|---|---|---|---|---|---|---|
| $^{220}_{90}\text{Th}_{130}$ | 0.769 | 0.874 | $^{16}_{8}\text{O} + ^{204}_{82}\text{Pb}$ | 76.30 | −44.516 | 656 | 0.439 | 0.855 | 0.60 | [45,115,116] |
| | | | $^{40}_{18}\text{Ar} + ^{180}_{72}\text{Hf}$ | 142.63 | −99.491 | 1296 | 0.618 | 0.636 | 0.05 | [117,118] |
| | | | $^{48}_{20}\text{Ca} + ^{172}_{70}\text{Yb}$ | 152.47 | −118.150 | 1400 | 0.629 | 0.564 | 0.03[a] | [27] |
| | | | $^{70}_{30}\text{Zn} + ^{150}_{60}\text{Nd}$ | 192.32 | −157.913 | 1800 | 0.728 | 0.364 | 0.002[a] | [119] |
| | | | $^{82}_{34}\text{Se} + ^{138}_{56}\text{Ba}$ | 202.19 | −180.525 | 1904 | 0.745 | 0.255 | 0.01 | [51] |
| | | | $^{124}_{50}\text{Sn} + ^{96}_{40}\text{Zr}$ | 211.50 | −188.348 | 2000 | 0.765 | 0.127 | 0.005 | [27,120] |

[a]Experimental $\sigma_{\Sigma xn}$ have been used instead of $\sigma_{ER}$.

in the extracted $\langle P_{CN} \rangle$ values presented in this article, are insignificant.

Results of the SM calculation may also be susceptible to uncertainties, particularly when major conclusions are drawn based on data from a handful of systems. There are scopes of ambiguity in choosing important SM parameters, e.g., fission barrier, level density parameters in the ground state ($a_n$), and at the saddle point ($a_f$), magnitude of shell effects, the rate at which shell effects disappear, etc. To ensure that our conclusions are robust, we have performed SM calculations for 52 reactions *without* adjusting any parameter to suit a particular reaction. Our model calculation reproduces measured ER excitation functions for 11 reactions with $A_{CN} \leqslant 200$ (cases with $\langle P_{CN} \rangle = 1$ in Table I).

Liang *et al.* [123] extracted fusion probability for a number of neutron-rich radioactive-Sn-induced reactions. The authors performed the SM calculation using PACE2 [124]. Four different sets of SM parameters, viz., inverse level density parameter ($k = \frac{A}{a}$), $\frac{a_f}{a_n}$, and diffuseness of the spin distribution ($\Delta\ell$), were considered. It was found that $\langle P_{CN} \rangle$ values changed maximum upto 16%, but the overall trend of $\langle P_{CN} \rangle \simeq 1$ with respect to $\chi_{eff}$ remained the same. Based on our SM calculation and the work of Liang *et al.*, we may conclude that the presented $\langle P_{CN} \rangle$ values are free from any large uncertainties that may arise because of ambiguity in choosing SM parameters.

It may be remarked here that use of free energy to provide the driving force in fission had been advocated earlier [125,126]. The fission barrier in free energy profile is temperature-dependent and is smaller than that in potential energy profile [126]. Consequently, the fission width from free energy is larger than that from potential energy consideration. Thus $\sigma_{ER}^{max}$ calculated with the free energy fission barrier is expected to be smaller than that obtained with the potential
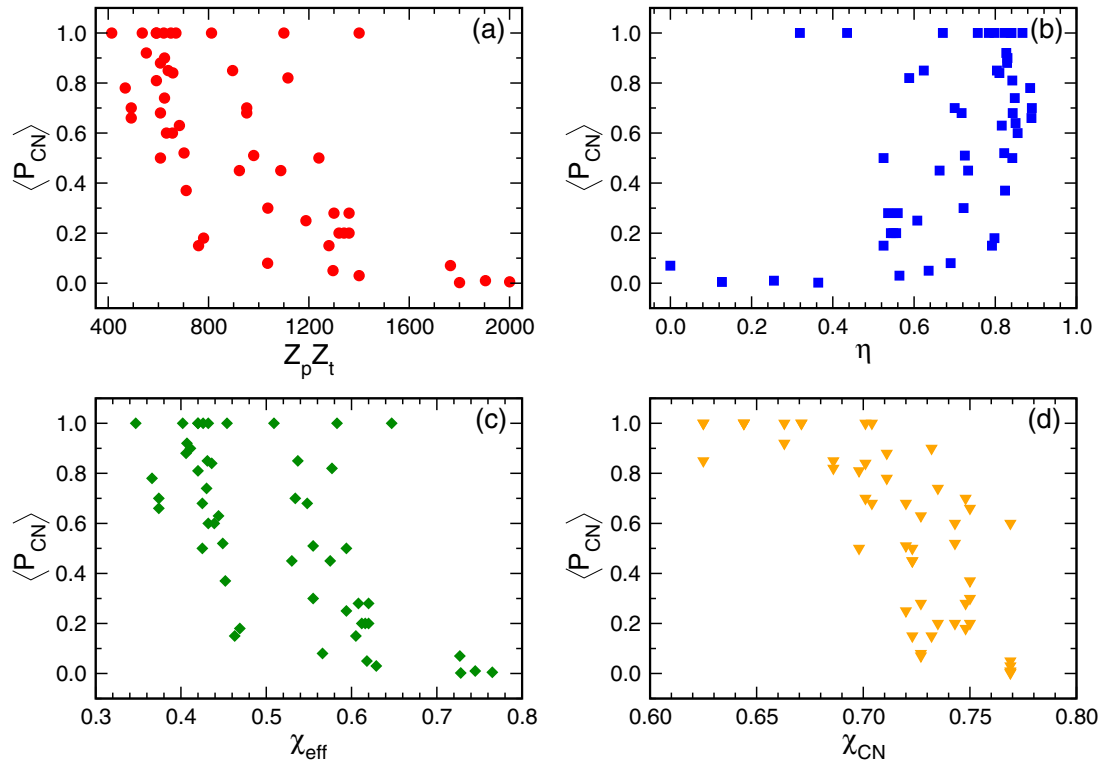


FIG. 6. (Color online) Variation of $\langle P_{CN} \rangle$ as a function of (a) $Z_p Z_t$, (b) $\eta$, (c) $\chi_{eff}$, and (d) $\chi_{CN}$. See text for details.
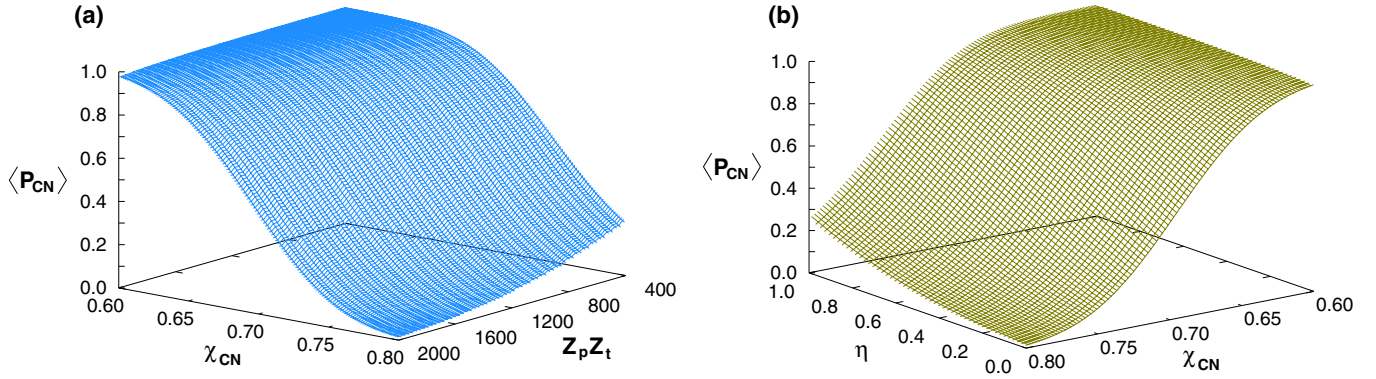
FIG. 7. (Color online) $\langle P_{CN} \rangle$ surface plots as a function of (a) $Z_p Z_t$ and $\chi_{CN}$, (b) $\eta$ and $\chi_{CN}$.

energy fission barrier. This, in turn, may yield larger values of $\langle P_{CN} \rangle$ for several reactions listed in Table I. As a consequence, the straight lines shown in Fig. 8 may be pushed somewhat upwards, i.e., towards larger $\chi_{CN}$. We plan to carry out such an analysis in a future work. However, this eventuality does not alter the larger point that we are making in this article.

Our method of scaling down calculated ER excitation function onto the measured ER excitation function may also add uncertainties in the extracted $\langle P_{CN} \rangle$ values. Systems for which data points are available over the entire region of interest (shaded regions in Fig. 3–5), "fitting errors" are estimated to be ∼10%. For systems with only a few data points (e.g., $^{48}$Ca + $^{154}$Gd, $^{22}$Ne + $^{190}$Os, etc.), fitting errors could be as high as ∼20%.

We must be aware of another source of uncertainties in our extracted values of $\langle P_{CN} \rangle$. Experimental data have been taken from the literature and SM results have been scaled down to match data points to get $\langle P_{CN} \rangle$. Since these experiments had been performed in different facilities and with varied setups, different data sets may have unknown sources of systematic errors. This has been evident in a number of instances in which two data sets for the same reaction did not agree with each other. Though we have matched SM predictions with data points in each case in an unbiased manner, additional uncertainties (besides those discussed already) due to systematic errors in measured $\sigma_{ER}$ cannot be ruled out completely. This is probably the reason

that about a quarter of the systems exhibit different trends of $\langle P_{CN} \rangle$ compared to the rest.

Several authors [63,106,108,113,127–131] had reported suppression of measured ER excitation function with respect to the same obtained from the SM calculation. The data, in such cases, were fitted by scaling down the liquid drop fission barrier by a "scaling factor" (usually denoted by $k_f$). This approach appears to be arbitrary as its sole purpose was to fit the data at hand. No efforts were made to obtain a global prescription for the scaling factor. Also, the role of $P_{CN}$ in suppressing $\sigma_{ER}$ was neglected altogether. This article contends that non-negligible contribution from $P_{CN}$ should be accounted for in such cases.

Very recently, Schmitt *et al.* [132] have examined a set of experimental observables from the reactions $^{12}$C + $^{194,198}$Pt → $^{206,210}$Po using a Langevin dynamical calculation with dissipation in multidimensional free energy profile. Considerable ambiguity in the interpretation of experimental observables, based solely on the SM calculation, has been highlighted in this work. The authors have argued that extraction of fundamental properties of nuclei based on conventional SM analysis may not be reliable, and the role of dynamics in interpreting experimental observables from fissile systems is non-negligible. Our findings, broadly speaking, convey a similar message. In addition, we present approximate limits on the applicability of SM to analyze experimental observables emanating from fusion between two massive nuclei.
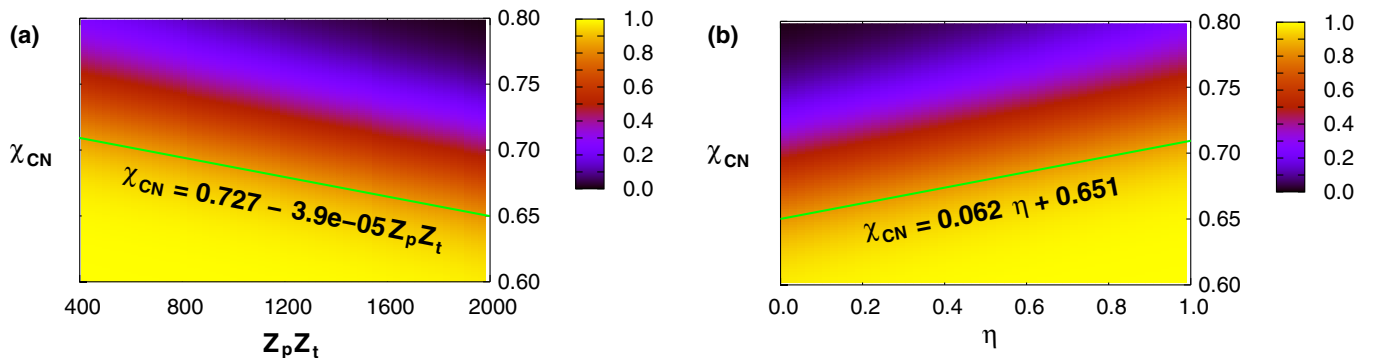


FIG. 8. (Color online) Projection of $\langle P_{CN} \rangle$ surface plots (shown in Fig. 7) on the (a) $Z_p Z_t$–$\chi_{CN}$ and (b) $\eta$–$\chi_{CN}$ planes. Variation of $\langle P_{CN} \rangle$ is shown with a color gradient. The two straight lines denote the "boundaries" between the regions with $\langle P_{CN} \rangle = 1$ and $\langle P_{CN} \rangle < 1$.

Finally, we focus on the possible correlation between fusion suppression (i.e., $\langle P_{CN} \rangle < 1$) and $\eta_{BG}$. The literature abounds with numerous instances (e.g., Ref. [133]) when $\eta_{BG}$ has been assumed to play a decisive role in the appearance of NCNF. We find from our analysis that this is only approximately true. Systems leading to $A_{CN} \leqslant 190$ show $\langle P_{CN} \rangle \sim 1$, even though some of these reactions have $\eta < \eta_{BG}$. The reactions $^{12}\text{C} + ^{204,206}\text{Pb} \rightarrow ^{216,218}\text{Ra}$ have $\eta > \eta_{BG}$, but $\langle P_{CN} \rangle$ in both the cases are substantially lower than unity. Sagaidak *et al.* [134] reported a search for the "starting point" of NCNF in fissile nuclei in an attempt to correlate $P_{CN}$ with $\eta_{BG}$. With the limited number of reactions that were analyzed in this work, the authors obtained only *indirect evidence* for a decisive role of $\eta_{BG}$ in the presence of NCNF in a reaction.

## V. SUMMARY AND CONCLUSIONS

We have examined $\sigma_{ER}$, obtained in fusion reactions between two massive nuclei, for 52 systems leading to CN with mass 170–220. We have calculated $\sigma_{cap}$ for these reactions using the coupled-channels code CCFULL. For consistency, Woods-Saxon parametrization of the Akyüz-Winther potential has been used in all cases. Distributions of $\sigma_\ell$ for each reaction, generated by CCFULL, have been fed as the input to an SM code to get theoretical ER excitation function. We have followed the transition-state model of Bohr and Wheeler for fission and used the FRLDM fission barrier. Shell corrections have been included in both the level density and the fission barrier.

Experimental nuclear masses have been used to calculate particle separation energies. We have attributed the difference between measured and calculated ER excitation functions to the presence of NCNF which causes hindrance to the formation of an equilibrated CN. $\langle P_{CN} \rangle$ for each reaction has been determined by comparing measured and calculated $\sigma_{ER}$. We have focused in the region $\frac{E_{c.m.}}{V_B} \sim 1.05$–$1.35$, where known nuclear structure effects may not be significant. Also, this is the region of interest for synthesis of SHE. Our systematic analysis revealed that $\langle P_{CN} \rangle$ depends both on the entrance channel parameters ($Z_p Z_t$ or $\eta$) and the bulk properties of the composite system ($\chi_{CN}$). We have also found out approximate boundaries from where $\langle P_{CN} \rangle$ starts deviating from unity. This is very important as the same denote the limits of validity of the SM in describing fusion observables in the heavy mass region. One should opt for a suitable dynamical model for fusion beyond these approximate limits. Results from several fusion reactions, leading to CN in the mass region 200 and above, had been reported earlier where experimental observables had been interpreted solely on the basis of the SM. In the light of our findings and those of Ref. [132], we strongly feel that such results should be looked into afresh.

## ACKNOWLEDGMENT

[1] J. H. Hamilton, S. Hofmann, and Y. T. Oganessian, Annu. Rev. Nucl. Part. Sci. **63**, 383 (2013).

[2] N. Bohr, Nature (London) **137**, 344 (1936).

[3] O. Hahn and F. Strassmann, Naturwissenschaften **27**, 11 (1939).

[4] N. Rowley and N. S. Grar, EPJ Web Conf. **17**, 09004 (2011).

[5] V. I. Zagrebaev, Y. Aritomo, M. G. Itkis, Yu. Ts. Oganessian, and M. Ohta, Phys. Rev. C **65**, 014607 (2001).

[6] B. Borderie, M. Berlanger, D. Gardès, F. Hanappe, L. Nowicki, J. Péter, B. Tamain, S. Agarwal, J. Girard, C. Grégoire, J. Matuszek, and C. Ngô, Z. Phys. A **299**, 263 (1981).

[7] J. Tōke, R. Bock, G. X. Dai, A. Gobbi, S. Gralla, K. D. Hildenbrand, J. Kuzminski, W. F. J. Müller, A. Olmi, H. Stelzer, B. B. Back, and S. Bjørnholm, Nucl. Phys. A **440**, 327 (1985).

[8] V. S. Ramamurthy and S. S. Kapoor, Phys. Rev. Lett. **54**, 178 (1985).

[9] W. J. Światecki, Phys. Scr. **24**, 113 (1981).

[10] S. Bjørnholm and W. J. Światecki, Nucl. Phys. A **391**, 471 (1982).

[11] J. Blocki, H. Feldmeier, and W. J. Światecki, Nucl. Phys. A **459**, 145 (1986).

[12] N. V. Antonenko, E. A. Cherepanov, A. K. Nasirov, V. P. Permjakov, and V. V. Volkov, Phys. Lett. B **319**, 425 (1993).

[13] N. V. Antonenko, E. A. Cherepanov, A. K. Nasirov, V. P. Permjakov, and V. V. Volkov, Phys. Rev. C **51**, 2635 (1995).

[14] G. G. Adamian, N. V. Antonenko, W. Scheid, and V. V. Volkov, Nucl. Phys. A **627**, 361 (1997).

[15] G. G. Adamian, N. V. Antonenko, and W. Scheid, Nucl. Phys. A **678**, 24 (2000).

[16] A. K. Nasirov, G. Mandaglio, G. Giardina, A. Sobiczewski, and A. I. Muminov, Phys. Rev. C **84**, 044612 (2011).

[17] N. Wang, E.-G. Zhao, W. Scheid, and S.-G. Zhou, Phys. Rev. C **85**, 041601 (2012).

[18] V. I. Zagrebaev, Phys. Rev. C **64**, 034606 (2001).

[19] A. Diaz-Torres, Phys. Rev. C **69**, 021603 (2004).

[20] A. Diaz-Torres, Phys. Rev. C **74**, 064601 (2006).

[21] W. J. Światecki, K. Siwek-Wilczyńska, and J. Wilczyński, Phys. Rev. C **71**, 014602 (2005).

[22] T. Cap, K. Siwek-Wilczyńska, and J. Wilczyński, Phys. Rev. C **83**, 054602 (2011).

[23] K. Siwek-Wilczyńska, T. Cap, M. Kowal, A. Sobiczewski, and J. Wilczyński, Phys. Rev. C **86**, 014611 (2012).

[24] Y. Aritomo, T. Wada, M. Ohta, and Y. Abe, Phys. Rev. C **59**, 796 (1999).

[25] Y. Aritomo, K. Hagino, K. Nishio, and S. Chiba, Phys. Rev. C **85**, 044614 (2012).

[26] A. Kaur, S. Chopra, and R. K. Gupta, Phys. Rev. C **90**, 024619 (2014).

[27] C.-C. Sahm, H.-G. Clerc, K.-H. Schmidt, W. Reisdorf, P. Armbruster, F. P. Heßberger, J. G. Keller, G. Münzenberg, and D. Vermeulen, Nucl. Phys. A **441**, 316 (1985).

[28] J. Blocki, L. Shvedov, and J. Wilczyński, Int. J. Mod. Phys. E **15**, 426 (2006).

[29] K. Siwek-Wilczyńska, A. Borowiec, I. Skwira-Chalot, and J. Wilczyński, Int. J. Mod. Phys. E **17**, 12 (2008).

[30] V. I. Zagrebaev and W. Greiner, Phys. Rev. C **78**, 034610 (2008).

[31] N. Wang, J. Tian, and W. Scheid, Phys. Rev. C **84**, 061601 (2011).

[32] R. N. Sagaidak, EPJ Web Conf. **21**, 06001 (2012).

[33] R. Yanez, W. Loveland, J. S. Barrett, L. Yao, B. B. Back, S. Zhu, and T. L. Khoo, Phys. Rev. C **88**, 014606 (2013).

[34] R. S. Naik, W. Loveland, P. H. Sprunger, A. M. Vinodkumar, D. Peterson, C. L. Jiang, S. Zhu, X. Tang, E. F. Moore, and P. Chowdhury, Phys. Rev. C **76**, 054604 (2007).

[35] B. B. Back, Phys. Rev. C **31**, 2104 (1985).

[36] J. G. Keller, B. B. Back, B. G. Glagola, D. Henderson, S. B. Kaufman, S. J. Sanders, R. H. Siemssen, F. Videbaek, B. D. Wilkins, and A. Worsham, Phys. Rev. C **36**, 1364 (1987).

[37] E. M. Kozulin *et al.*, Phys. Lett. B **686**, 227 (2010).

[38] I. M. Itkis, E. M. Kozulin, M. G. Itkis, G. N. Knyazheva, A. A. Bogachev, E. V. Chernysheva, L. Krupa, Yu. Ts. Oganessian, V. I. Zagrebaev, A. Ya. Rusanov, F. Goennenwein, O. Dorvaux, L. Stuttgé, F. Hanappe, E. Vardaci, and E. de Goés Brennand, Phys. Rev. C **83**, 064613 (2011).

[39] K. Nishio, S. Mitsuoka, I. Nishinaka, H. Makii, Y. Wakabayashi, H. Ikezoe, K. Hirose, T. Ohtsuki, Y. Aritomo, and S. Hofmann, Phys. Rev. C **86**, 034608 (2012).

[40] G. N. Knyazheva *et al.*, Phys. Rev. C **75**, 064602 (2007).

[41] S. Soheyli and M. K. Khalili, Phys. Rev. C **85**, 034610 (2012).

[42] R. K. Choudhury and R. G. Thomas, J. Phys. Conf. Ser. **282**, 012004 (2011).

[43] R. du Rietz, E. Williams, D. J. Hinde, M. Dasgupta, M. Evers, C. J. Lin, D. H. Luong, C. Simenel, and A. Wakhle, Phys. Rev. C **88**, 054618 (2013).

[44] A. C. Berriman, D. J. Hinde, M. Dasgupta, C. R. Morton, R. D. Butt, and J. O. Newton, Nature (London) **413**, 144 (2001).

[45] D. J. Hinde, M. Dasgupta, and A. Mukherjee, Phys. Rev. Lett. **89**, 282701 (2002).

[46] A. M. Stefanini *et al.*, Eur. Phys. J. A **23**, 473 (2005).

[47] D. J. Hinde and M. Dasgupta, Phys. Lett. B **622**, 23 (2005).

[48] J. G. Keller, K.-H. Schmidt, F. P. Heßberger, G. Münzenberg, W. Reisdorf, H.-G. Clerc, and C.-C. Sahm, Nucl. Phys. A **452**, 173 (1986).

[49] K.-H. Schmidt and W. Morawek, Rep. Prog. Phys. **54**, 949 (1991).

[50] A. B. Quint, W. Reisdorf, K.-H. Schmidt, P. Armbruster, F. P. Heßberger, S. Hofmann, J. Keller, G. Münzenberg, H. Stelzer, H.-G. Clerc, W. Morawek, and C.-C. Sahm, Z. Phys. A **346**, 119 (1993).

[51] K. Satou, H. Ikezoe, S. Mitsuoka, K. Nishio, and S. C. Jeong, Phys. Rev. C **65**, 054602 (2002).

[52] P. D. Shidling, N. M. Badiger, S. Nath, R. Kumar, A. Jhingan, R. P. Singh, P. Sugathan, S. Muralithar, N. Madhavan, A. K. Sinha, S. Pal, S. Kailas, S. Verma, K. Kalita, S. Mandal, R. Singh, B. R. Behera, K. M. Varier, and M. C. Radhakrishna, Phys. Rev. C **74**, 064603 (2006).

[53] K. Hagino, N. Rowley, and A. T. Kruppa, Comput. Phys. Commun. **123**, 143 (1999).

[54] J. Sadhukhan and S. Pal, Phys. Rev. C **81**, 031602 (2010).

[55] P. Fröbrich and I. I. Gontchar, Phys. Rep. **292**, 131 (1998).

[56] N. Bohr and J. A. Wheeler, Phys. Rev. **56**, 426 (1939).

[57] V. M. Strutinsky, Phys. Lett. B **47**, 121 (1973).

[58] A. Bohr and B. R. Mottelson, *Nuclear Structure*, Vol. I (W. A. Benjamin, New York, 1996).

[59] A. V. Ignatyuk, M. G. Itkis, V. N. Okolovich, G. N. Smirenkin, and A. Tishin, Sov. J. Nucl. Phys. **21**, 255 (1975).

[60] W. Reisdorf, Z. Phys. A **300**, 227 (1981).

[61] A. J. Sierk, Phys. Rev. C **33**, 2039 (1986).

[62] Y. Aritomo, Nucl. Phys. A **780**, 222 (2006).

[63] V. Singh, B. R. Behera, M. Kaur, A. Kumar, K. P. Singh, N. Madhavan, S. Nath, J. Gehlot, G. Mohanto, A. Jhingan, I. Mukul, T. Varughese, J. Sadhukhan, S. Pal, S. Goyal, A. Saxena, S. Santra, and S. Kailas, Phys. Rev. C **89**, 024609 (2014).

[64] R. A. Broglia and A. Winther, *Heavy Ion Physics*, Part I and Part II (Addison-Wesley Publishing, Redwood City, CA, 1991).

[65] G. Audi, M. Wang, A. H. Wapstra, F. G. Kondev, M. MacCormick, X. Xu, and B. Pfeiffer, Chin. Phys. C **36**, 1287 (2012).

[66] S. Gil, F. Hasenbalg, J. E. Testoni, D. Abriola, M. C. Berisso, M. di Tada, A. Etchegoyen, J. O. Fernández Niello, A. J. Pacheco, A. Charlop, A. A. Sonzogni, and R. Vandenbosch, Phys. Rev. C **51**, 1336 (1995).

[67] F. Plasil, T. C. Awes, B. Cheynis, D. Drain, R. L. Ferguson, F. E. Obenshain, A. J. Sierk, S. G. Steadman, and G. R. Young, Phys. Rev. C **29**, 1145(R) (1984).

[68] K. Kumar, T. Ahmad, S. Ali, I. A. Rizvi, A. Agarwal, R. Kumar, K. S. Golda, and A. K. Chaubey, Phys. Rev. C **87**, 044608 (2013).

[69] A. Sharma, B. Bindu Kumar, S. Mukherjee, S. Chakrabarty, B. S. Tomar, A. Goswami, G. K. Gubbi, S. B. Manohar, A. K. Sinha, and S. K. Datta, Pramana–J. Phys. **54**, 355 (2000).

[70] P. P. Singh, B. P. Singh, M. K. Sharma, Unnati, D. P. Singh, R. Prasad, R. Kumar, and K. S. Golda, Phys. Rev. C **77**, 014607 (2008).

[71] D. Singh, R. Ali, M. Afzal Ansari, B. S. Tomar, M. H. Rashid, R. Guin, and S. K. Das, Nucl. Phys. A **879**, 107 (2012).

[72] R. J. Charity, J. R. Leigh, J. J. M. Bokhorst, A. Chatterjee, G. S. Foote, D. J. Hinde, J. O. Newton, S. Ogaza, and D. Ward, Nucl. Phys. A **457**, 441 (1986).

[73] W. S. Freeman, H. Ernst, D. F. Geesaman, W. Henning, T. J. Humanic, W. Kühn, G. Rosner, J. P. Schiffer, B. Zeidman, and F. W. Prosser, Phys. Rev. Lett. **50**, 1563 (1983).

[74] K. T. Lesko, W. Henning, K. E. Rehm, G. Rosner, J. P. Schiffer, G. S. F. Stephans, B. Zeidman, and W. S. Freeman, Phys. Rev. C **34**, 2155 (1986).

[75] S. K. Hui, C. R. Bhuinya, A. K. Ganguly, N. Madhavan, J. J. Das, P. Sugathan, D. O. Kataria, S. Mutlithar, L. T. Baby, V. Tripathi, A. Jhingan, A. K. Sinha, P. V. Madhusudhana Rao, N. V. S. V. Prasad, A. M. VinodKumar, R. Singh, M. Thoennessen, and G. Gervais, Phys. Rev. C **62**, 054604 (2000).

[76] A. Chatterjee, A. Shrivastava, S. Kailas, A. Navin, P. Singh, S. K. Datta, T. Madhusoodhanan, S. Mandal, and M. K. Sharan, Proc. DAE Symp. Nucl. Phys. **39B**, 170 (1996).

[77] W. Reisdorf, F. P. Heßberger, K. D. Hildenbrand, S. Hofmann, G. Münzenberg, K.-H. Schmidt, J. H. R. Schneider, W. F. W. Schneider, K. Sümmerer, G. Wirth, J. V. Kratz, and K. Schlitt, Phys. Rev. Lett. **49**, 1811 (1982).

[78] W. Reisdorf, F. P. Heßberger, K. D. Hildenbrand, S. Hofmann, G. Münzenberg, K.-H. Schmidt, J. H. R. Schneider, W. F. W.

Schneider, K. Sümmerer, G. Wirth, J. V. Kratz, and K. Schlitt, Nucl. Phys. A **438**, 212 (1985).

[79] C. E. Beamis *et al.*, ORNL Physics Division Progress Report No. 6326, 1986 (unpublished), p. 110.

[80] J. R. Leigh, J. J. M. Bokhorst, D. J. Hinde, and J. O. Newton, J. Phys. G: Nucl. Phys. **14**, L55 (1988).

[81] D. J. Hinde, J. O. Newton, J. R. Leigh, and R. J. Charity, Nucl. Phys. A **398**, 308 (1983).

[82] D. J. Hinde, R. J. Charity, G. S. Foote, J. R. Leigh, J. O. Newton, S. Ogaza, and A. Chattejee, Nucl. Phys. A **452**, 550 (1986).

[83] J. S. Forster, I. V. Mitchell, J. U. Andersen, A. S. Jensen, E. Laegsgaard, W. M. Gibson, and K. Reichelt, Nucl. Phys. A **464**, 497 (1987).

[84] D. J. Hinde, J. R. Leigh, J. O. Newton, W. Galster, and S. Sie, Nucl. Phys. A **385**, 109 (1982).

[85] A. N. Andreyev, D. D. Bogdanov, V. I. Chepigin, A. P. Kabachenko, O. N. Malyshev, Yu. A. Muzichka, A. G. Popeko, B. I. Pustylnik, R. N. Sagaidak, G. M. Ter-Akopian, and A. V. Yeremin, Nucl. Phys. A **583**, 169 (1995).

[86] W. Morawek, D. Ackermann, T. Brohm, H.-G. Clerc, U. Gollerthan, E. Hanelt, M. Horz, W. Schwab, B. Voss, K.-H. Schmidt, and F. P. Heßberger, Z. Phys. A **341**, 75 (1991).

[87] R. C. Lemmon, J. R. Leigh, J. X. Wei, C. R. Morton, D. J. Hinde, J. O. Newton, J. C. Mein, M. Dasgupta, and N. Rowley, Phys. Lett. B **316**, 32 (1993).

[88] J. R. Leigh, M. Dasgupta, D. J. Hinde, J. C. Mein, C. R. Morton, R. C. Lemmon, J. P. Lestone, J. O. Newton, H. Timmers, J. X. Wei, and N. Rowley, Phys. Rev. C **52**, 3151 (1995).

[89] M. Trotta *et al.*, Nucl. Phys. A **734**, 245 (2004).

[90] R. Rafiei, R. G. Thomas, D. J. Hinde, M. Dasgupta, C. R. Morton, L. R. Gasques, M. L. Brown, and M. D. Rodriguez, Phys. Rev. C **77**, 024606 (2008).

[91] C. R. Morton, A. C. Berriman, R. D. Butt, M. Dasgupta, A. Godley, D. J. Hinde, and J. O. Newton, Phys. Rev. C **62**, 024607 (2000).

[92] C. R. Morton, D. J. Hinde, A. C. Berriman, R. D. Butt, M. Dasgupta, A. Godley, and J. O. Newton, Phys. Lett. B **481**, 160 (2000).

[93] D. A. Mayorov, T. A. Werke, M. C. Alfonso, M. E. Bennett, and C. M. Folden III, Phys. Rev. C **90**, 024602 (2014).

[94] R. Tripathi, K. Sudarshan, S. K. Sharma, S. Sodaye, A. V. R. Reddy, and A. Goswami, Proc. DAE Symp. Nucl. Phys. **53**, 387 (2008).

[95] J. van der Plicht, H. C. Britt, M. M. Fowler, Z. Fraenkel, A. Gavron, J. B. Wilhelmy, F. Plasil, T. C. Awes, and G. R. Young, Phys. Rev. C **28**, 2022 (1983).

[96] K. Sudarshan, R. Tripathi, S. Sodaye, S. K. Sharma, P. K. Pujari, J. Gehlot, N. Madhavan, S. Nath, G. Mohanto, I. Mukul, A. Jhingan, and I. Mazumdar, 75 Years of Nuclear Fission: Present Status and Future Perspectives, BARC, Mumbai, India, May 8-10, 2014, http://sympnp.org/proceedings/00/A13.pdf

[97] B. Tamain, C. Ngô, J. Péter, and F. Hanappe, Nucl. Phys. A **252**, 187 (1975).

[98] H. Delagrange, D. Logan, M. F. Rivet, M. Rajagopalan, J. M. Alexander, M. S. Zisman, M. Kaplan, and J. W. Ball, Phys. Rev. Lett. **43**, 1490 (1979).

[99] D. Logan, H. Delagrange, M. F. Rivet, M. Rajagopalan, J. M. Alexander, M. Kaplan, M. S. Zisman, and E. Duek, Phys. Rev. C **22**, 1080 (1980).

[100] K. Mahata, S. Kailas, A. Shrivastava, A. Chatterjee, A. Navin, P. Singh, S. Santra, and B. S. Tomar, Nucl. Phys. A **720**, 209 (2003).

[101] A. Shrivastava, S. Kailas, A. Chatterjee, A. M. Samant, A. Navin, P. Singh, and B. S. Tomar, Phys. Rev. Lett. **82**, 699 (1999).

[102] A. Shrivastava, S. Kailas, A. Chatterjee, A. Navin, A. M. Samant, P. Singh, S. Santra, K. Mahata, B. S. Tomar, and G. Pollarolo, Phys. Rev. C **63**, 054602 (2001).

[103] E. Prasad, K. M. Varier, N. Madhavan, S. Nath, J. Gehlot, S. Kalkal, J. Sadhukhan, G. Mohanto, P. Sugathan, A. Jhingan, B. R. S. Babu, T. Varughese, K. S. Golda, B. P. Ajith Kumar, B. Satheesh, S. Pal, R. Singh, A. K. Sinha, and S. Kailas, Phys. Rev. C **84**, 064606 (2011).

[104] E. Prasad, K. M. Varier, R. G. Thomas, A. M. Vinodkumar, K. Mahata, S. Appannababu, P. Sugathan, K. S. Golda, B. R. S. Babu, A. Saxena, B. V. John, and S. Kailas, Nucl. Phys. A **882**, 62 (2012).

[105] E. Prasad, P. V. Laveen, N. Madhavan, S. Nath, J. Gehlot, K. M. Varier, A. Jhingan, A. M. Vinodkumar, A. Shamlath, B. R. S. Babu, B. R. Behera, R. Sandal, V. Singh, J. Sadhukhan, S. Pal, and S. Kailas, Proc. DAE Symp. Nucl. Phys. **58**, 534 (2013).

[106] A. N. Andreyev, D. D. Bogdanov, V. I. Chepigin, A. P. Kabachenko, O. N. Malyshev, Yu. Ts. Oganessian, A. G. Popeko, J. Roháč, R. N. Sagaidak, G. M. Ter-Akopian, A. V. Yeremin, Š. Šáro, and M. Veselský, Nucl. Phys. A **626**, 857 (1997).

[107] S. Baba, K. Hata, S. Ichikawa, T. Sekine, Y. Nagame, A. Yokoyama, T. Shoji, T. Saito, N. Takahashi, H. Baba, and I. Fujiwara, Z. Phys. A **331**, 53 (1988).

[108] K.-T. Brinkmann, A. L. Caraley, B. J. Fineman, N. Gan, J. Velkovska, and R. L. McGrath, Phys. Rev. C **50**, 309 (1994).

[109] T. Sikkeland, Phys. Rev. **135**, B669 (1964).

[110] B. B. Back, C. L. Jiang, R. V. F. Janssens, D. J. Henderson, B. R. Shumard, C. J. Lister, D. Peterson, K. E. Rehm, I. Tanihata, X. Tang, X. Wang, and S. Zhu, in *FUSION06: Reaction Mechanisms and Nuclear Structure at the Coulomb Barrier, March 2006, San Servolo, Venezia, Italy*, edited by L. Corradi, D. Ackermann, E. Fioretto, A. Gadea, F. Haas, G. Pollarolo, F. Scarlassara, S. Szilner, and M. Trotta, AIP Conf. Proc. No. 853 (AIP, New York, 2006), p. 331.

[111] K. Mahata, S. Kailas, A. Shrivastava, A. Chatterjee, P. Singh, S. Santra, and B. S. Tomar, Phys. Rev. C **65**, 034613 (2002).

[112] D. J. Hinde, A. C. Berriman, R. D. Butt, M. Dasgupta, I. I. Gontchar, C. R. Morton, A. Mukherjee, and J. O. Newton, J. Nucl. Radiochem. Sci. **3**, 31 (2002).

[113] R. N. Sagaidak *et al.*, Phys. Rev. C **68**, 014603 (2003).

[114] A. N. Andreyev, D. D. Bogdanov, V. I. Chepigin, A. P. Kabachenko, O. N. Malyshev, Yu. A. Muzichka, Yu. Ts. Oganessian, A. G. Popeko, B. I. Pustylnik, R. N. Sagaidak, G. M. Ter-Akopian, and A. V. Yeremin, Nucl. Phys. A **620**, 229 (1997).

[115] H. Ikezoe, K. Satou, S. Mitsuoka, K. Nishio, K. Tsuruta, S. C. Jeong, and C. J. Lin, in *Tours Symposium on Nuclear Physics V, August 2003, Tours, France*, edited by M. Arnould, M. Lewitowicz, G. Münzenberg, H. Akimune, M. Ohta, H. Utsunomiya, T. Wada, and T. Yamagata, AIP Conf. Proc. No. 704 (AIP, New York, 2004), p. 73.

[116] M. Dasgupta, D. J. Hinde, A. Diaz-Torres, B. Bouriquet, C. I. Low, G. J. Milburn, and J. O. Newton, Phys. Rev. Lett. **99**, 192701 (2007).

[117] D. Vermeulen, H.-G. Clerc, C.-C. Sahm, K.-H. Schmidt, J. G. Keller, G. Münzenberg, and W. Reisdorf, Z. Phys. A **318**, 157 (1984).

[118] H.-G. Clerc, J. G. Keller, C.-C. Sahm, K.-H. Schmidt, H. Schulte, and D. Vermeulen, Nucl. Phys. A **419**, 571 (1984).

[119] C. Stodel, Ph.D. thesis, LPC Caen, LPC-C T98-05, 1998 (unpublished).

[120] A. M. Vinodkumar, W. Loveland, P. H. Sprunger, D. Peterson, J. F. Liang, D. Shapira, R. L. Varner, C. J. Gross, and J. J. Kolata, Phys. Rev. C **74**, 064612 (2006).

[121] U. L. Businaro and S. Gallone, Nuovo Cimento **5**, 315 (1957).

[122] W. Loveland, J. Phys: Conf. Ser. **420**, 012004 (2013).

[123] J. F. Liang, C. J. Gross, Z. Kohley, D. Shapira, R. L. Varner, J. M. Allmond, A. L. Caraley, K. Lagergren, and P. E. Mueller, Phys. Rev. C **85**, 031601 (2012).

[124] A. Gavron, Phys. Rev. C **21**, 230 (1980).

[125] A. Bohr and B. R. Mottelson, *Nuclear Structure*, Vol. II (W. A. Benjamin, New York, 1975).

[126] J. P. Lestone and S. G. McCalla, Phys. Rev. C **79**, 044611 (2009).

[127] G. Mohanto, N. Madhavan, S. Nath, J. Gehlot, I. Mukul, A. Jhingan, T. Varughese, A. Roy, R. K. Bhowmik, I. Mazumdar, D. A. Gothe, P. B. Chavan, J. Sadhukhan, S. Pal, M. Kaur, V. Singh, A. K. Sinha, and V. S. Ramamurthy, Phys. Rev. C **88**, 034606 (2013).

[128] L. Corradi, B. R. Behera, E. Fioretto, A. Gadea, A. Latina, A. M. Stefanini, S. Szilner, M. Trotta, Y. Wu, S. Beghini, G. Montagnoli, F. Scarlassara, R. N. Sagaidak, S. N. Atutov, B. Mai, G. Stancari, L. Tomassetti, E. Mariotti, A. Khanbekyan, and S. Veronesi, Phys. Rev. C **71**, 014609 (2005).

[129] A. N. Andreyev *et al.*, Phys. Rev. C **72**, 014612 (2005).

[130] R. N. Sagaidak and A. N. Andreyev, Phys. Rev. C **79**, 054613 (2009).

[131] S. Nath, P. V. Madhusudhana Rao, S. Pal, J. Gehlot, E. Prasad, G. Mohanto, S. Kalkal, J. Sadhukhan, P. D. Shidling, K. S. Golda, A. Jhingan, N. Madhavan, S. Muralithar, and A. K. Sinha, Phys. Rev. C **81**, 064601 (2010).

[132] C. Schmitt, K. Mazurek, and P. N. Nadtochy, Phys. Lett. B **737**, 289 (2014).

[133] P. D. Shidling, N. Madhavan, V. S. Ramamurthy, S. Nath, N. M. Badiger, S. Pal, A. K. Sinha, A. Jhingan, S. Muralithar, P. Sugathan, S. Kailas, B. R. Behera, R. Singh, K. M. Varier, and M. C. Radhakrishna, Phys. Lett. B **670**, 99 (2008).

[134] R. N. Sagaidak, A. Yu. Chizhov, I. M. Itkis, M. G. Itkis, G. N. Kniajeva, N. A. Kondratiev, E. M. Kozulin, I. V. Pokrovsky, L. Corradi, E. Fioretto, A. Gadea, A. Latina, A. M. Stefanini, S. Beghini, G. Montagnoli, F. Scarlassara, M. Trotta, and S. Szilner, in *FUSION06: Reaction Mechanisms and Nuclear Structure at the Coulomb Barrier, March 2006, San Servolo, Venezia, Italy*, edited by L. Corradi, D. Ackermann, E. Fioretto, A. Gadea, F. Haas, G. Pollarolo, F. Scarlassara, S. Szilner, and M. Trotta, AIP Conf. Proc. No. 853 (AIP, New York, 2006), p. 114.